NASA/TM-20210022054

Results From the MISSE 6 Scattered Space Atomic Oxygen Experiment (SSAOE)

Kim K. de Groh
Glenn Research Center, Cleveland, Ohio

Bruce A. Banks and Terry R. McCue
Science Applications International Corporation, Cleveland, Ohio

Curtis R. Stidham
Sverdrup Technology, Inc., Brook Park, Ohio

Scott R. Panko
Vantage Partners, LLC, Brook Park, Ohio

Olivia C. Asmar, Grace T. Yi, and Gianna G. Mitchell
Hathaway Brown School, Shaker Heights, Ohio

October 2021

NASA STI Program . . . in Profile

Since its founding, NASA has been dedicated to the advancement of aeronautics and space science. The NASA Scientific and Technical Information (STI) Program plays a key part in helping NASA maintain this important role.

The NASA STI Program operates under the auspices of the Agency Chief Information Officer. It collects, organizes, provides for archiving, and disseminates NASA's STI. The NASA STI Program provides access to the NASA Technical Report Server—Registered (NTRS Reg) and NASA Technical Report Server—Public (NTRS) thus providing one of the largest collections of aeronautical and space science STI in the world. Results are published in both non-NASA channels and by NASA in the NASA STI Report Series, which includes the following report types:

- TECHNICAL PUBLICATION. Reports of completed research or a major significant phase of research that present the results of NASA programs and include extensive data or theoretical analysis. Includes compilations of significant scientific and technical data and information deemed to be of continuing reference value. NASA counter-part of peer-reviewed formal professional papers, but has less stringent limitations on manuscript length and extent of graphic presentations.

- TECHNICAL MEMORANDUM. Scientific and technical findings that are preliminary or of specialized interest, e.g., "quick-release" reports, working papers, and bibliographies that contain minimal annotation. Does not contain extensive analysis.

- CONTRACTOR REPORT. Scientific and technical findings by NASA-sponsored contractors and grantees.

- CONFERENCE PUBLICATION. Collected papers from scientific and technical conferences, symposia, seminars, or other meetings sponsored or co-sponsored by NASA.

- SPECIAL PUBLICATION. Scientific, technical, or historical information from NASA programs, projects, and missions, often concerned with subjects having substantial public interest.

- TECHNICAL TRANSLATION. English-language translations of foreign scientific and technical material pertinent to NASA's mission.

For more information about the NASA STI program, see the following:

- Access the NASA STI program home page at http://www.sti.nasa.gov

- E-mail your question to help@sti.nasa.gov

- Fax your question to the NASA STI Information Desk at 757-864-6500

- Telephone the NASA STI Information Desk at 757-864-9658

- Write to:
  NASA STI Program
  Mail Stop 148
  NASA Langley Research Center
  Hampton, VA 23681-2199

NASA/TM-20210022054

Results From the MISSE 6 Scattered Space Atomic Oxygen Experiment (SSAOE)

Kim K. de Groh
Glenn Research Center, Cleveland, Ohio

Bruce A. Banks and Terry R. McCue
Science Applications International Corporation, Cleveland, Ohio

Curtis R. Stidham
Sverdrup Technology, Inc., Brook Park, Ohio

Scott R. Panko
Vantage Partners, LLC, Brook Park, Ohio

Olivia C. Asmar, Grace T. Yi, and Gianna G. Mitchell
Hathaway Brown School, Shaker Heights, Ohio

National Aeronautics and
Space Administration

Glenn Research Center
Cleveland, Ohio 44135

October 2021

Acknowledgments

We would like to express our sincere appreciation to NASA Langley Research Center and Gary H. Pippin, formerly of Boeing, for providing the opportunity to be a part of the MISSE 6 mission. We thank Donald Jaworske, formerly of NASA Glenn Research Center, for coordinating all the NASA Glenn MISSE 6 experiments. We would like to thank Patty Hunt, formerly of Hathaway Brown School, for her support of the NASA Glenn Research Center and Hathaway Brown School 20 year collaboration, which made it possible for the Hathaway Brown students to be a part of this project. We thank Craig Robinson of NASA Glenn Research Center for his encouragement and constant support of our MISSE flight experiments. Originally supported by various programs, this work is currently supported by the NASA Biological and Physical Sciences Division.

Level of Review: This material has been technically reviewed by technical management.

Available from

NASA STI Program
Mail Stop 148
NASA Langley Research Center
Hampton, VA 23681-2199

National Technical Information Service
5285 Port Royal Road
Springfield, VA 22161
703-605-6000

This report is available in electronic form at http://www.sti.nasa.gov/ and http://ntrs.nasa.gov/

Results From the MISSE 6 Scattered Space Atomic Oxygen Experiment (SSAOE)

Kim K. de Groh
National Aeronautics and Space Administration
Glenn Research Center
Cleveland, Ohio 44135

Bruce A. Banks and Terry R. McCue
Science Applications International Corporation
Cleveland, Ohio 44135

Curtis R. Stidham
Sverdrup Technology, Inc.
Brook Park, Ohio 44142

Scott R. Panko
Vantage Partners, LLC
Brook Park, Ohio 44142

Olivia C. Asmar, Grace T. Yi, and Gianna G. Mitchell
Hathaway Brown School
Shaker Heights, Ohio 44122

Abstract

Polymers and other oxidizable materials used on the exterior of spacecraft in the low Earth orbit (LEO) space environment can be eroded away by reaction with atomic oxygen (AO). NASA Glenn Research Center developed an active flight experiment, called the Scattered Space Atomic Oxygen Experiment (SSAOE), to characterize AO scattering erosion in space. The SSAOE is comprised of three independent sub-experiments: A two part active experiment to measure both in-situ direct ram AO erosion and in-situ scattered AO erosion within an AO scatterometer; a passive AO scatterometer to measure the angular distribution of LEO AO scattered off an inclined angle; and passive samples for AO erosion yield (E_y) characterization. The SSAOE was originally flown on the Wake Shield Facility (WSF) during the STS-60 shuttle mission, and was later flown as part of the MISSE 6 mission on the exterior of the ISS. During the MISSE-6 mission the SSAOE was exposed to the space environment for 1.45 years. This paper provides an overview of the SSAOE, information on the flight missions, post-flight photographs of the passive flight samples and results on the angular distribution of scattered LEO AO obtained from the passive AO scatterometer sub-experiment. The LEO scattered AO erosion data can be used to improve AO undercutting models and durability predictions of spacecraft components receiving scattered AO.

Introduction

Spacecraft in the low Earth orbit (LEO) environment (between 200 and 2000 km above the surface of the Earth) endure extremely harsh conditions, including exposure to visible light photon radiation, ultraviolet (UV) radiation, vacuum ultraviolet (VUV) radiation, x-rays, solar wind

particle radiation (electrons, protons), cosmic rays, temperature extremes, thermal cycling, impacts from micrometeoroids and orbital debris (MMOD), on-orbit contamination, and atomic oxygen (AO). These environmental exposures can result in erosion, embrittlement and optical property degradation of susceptible materials threatening spacecraft performance and durability.

Although all space environmental exposures can cause degradation to spacecraft components, AO is a particularly serious structural, thermal, and optical threat, especially to exterior oxidizable spacecraft components. Atomic oxygen is formed in the LEO environment through photodissociation of diatomic oxygen (O_2). Short-wavelength (<243 nm) solar radiation has sufficient energy to break the 5.12-eV O_2 diatomic bond in an environment where the mean free path is sufficiently long (~10^8 m) so that the probability of re-association, or the formation of ozone (O_3), is small.[1,2] In LEO, between the altitudes of 180 and 650 km, AO is the most abundant species.[3]

A number of processes can take place when an oxygen atom strikes a spacecraft surface as a result of its orbital velocity and the thermal velocity of the atoms. These include chemical reaction with surface molecules, elastic scattering, scattering with partial or full thermal accommodation, and recombination or excitation of ram species, which consists predominantly of ground-state $O(^3P)$ atomic oxygen atoms.[4] Atomic oxygen can react with polymers, carbon, and many metals to form oxygen bonds with atoms on the exposed surface. For most polymers, hydrogen abstraction, oxygen addition, or oxygen insertion can occur, with the oxygen interaction pathways eventually leading to volatile oxidation products.[5,6] This results in gradual erosion of hydrocarbon or halocarbon material, with the exception of silicone materials, which form a glassy silicate surface layer with AO exposure. Figure 1 shows AO erosion of Teflon™ fluorinated ethylene propylene (FEP) around a small protective particle after 5.8 years of space exposure on the Long Duration Exposure Facility (LDEF). An example of the complete loss of a Kapton® H thermal blanket insulation layer on the LDEF and degradation of other polymeric materials caused by AO erosion in LEO are provided in Figure 2.[2,7]

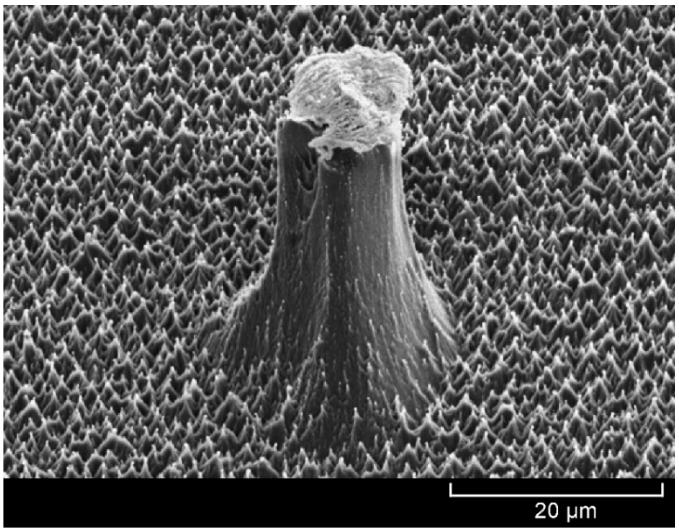

Figure 1. Atomic oxygen erosion of Teflon FEP after 5.8 years of space exposure.[2,7]

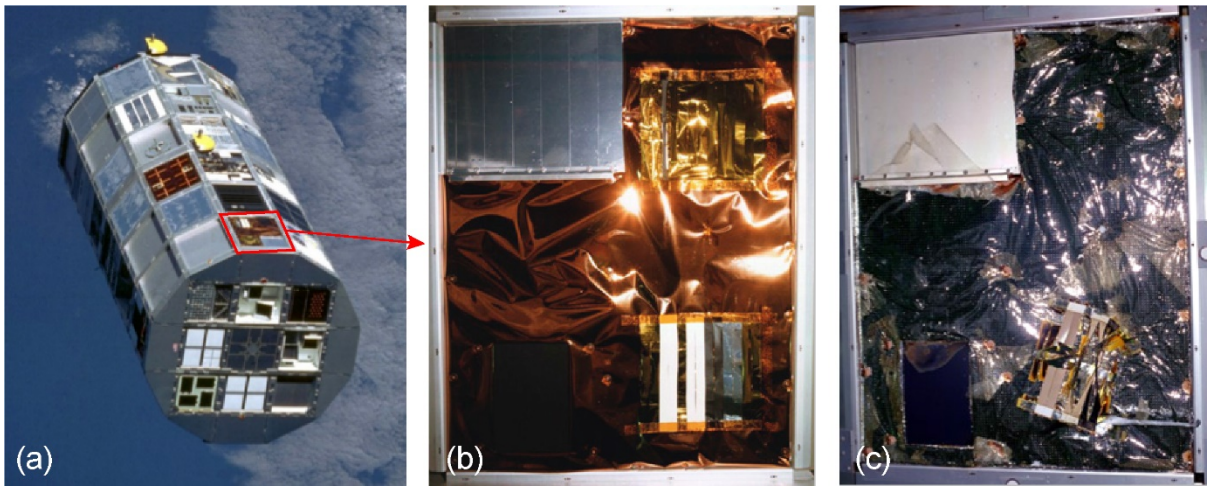

Figure 2. Atomic oxygen erosion of a Kapton insulation blanket from LDEF experiment Tray F-9, located on the leading edge and exposed to direct-ram AO for 5.8 years. (a) LDEF, (b) Tray F-9 pre-flight, and (c) Tray F-9 post-flight.[7]

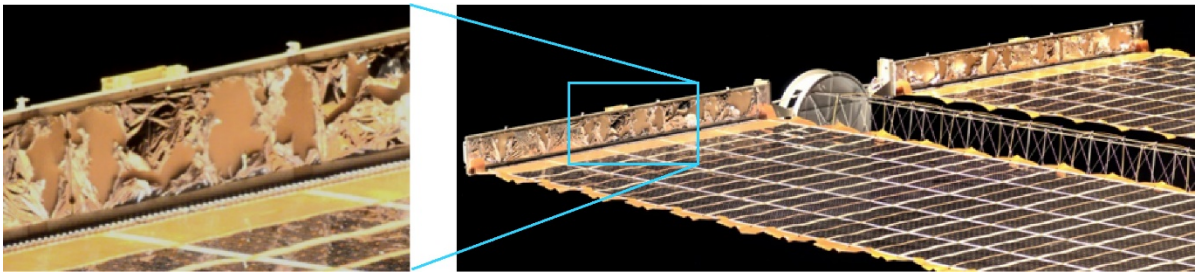

Figure 3. Atomic oxygen undercutting degradation of the P6 Truss solar array wing blanket box cover on the ISS after only 1 year of space exposure.[10]

Atomic oxygen scattering and subsequent reaction is a serious spacecraft durability concern. The most common approach to protecting susceptible spacecraft materials from AO erosion is to coat the material with a thin protective film, such as SiO_x (where x = 1.8 to 2). But, even materials with AO protective coatings can be susceptible to AO erosion as a result of microscopic scratches, dust particles, or other imperfections in the substrate surface, which can result in defects or pin windows in the protective coating.[8,9] These coating defects can provide pathways for AO attack, and undercutting erosion of the substrate can occur due to AO scattering and subsequent reactions, even under directed ram AO exposure in LEO. Atomic oxygen undercutting can result in cavities much larger than the size of the original defect site. One of the first examples of directed ram AO undercutting erosion in LEO was reported by de Groh and Banks for aluminized-Kapton insulation blankets from the LDEF.[8] Undercutting erosion can be a serious threat to component survivability. An example is shown in Figure 3, where AO undercutting erosion has severely degraded the P6 Truss port solar array wing two-surface aluminized-Kapton blanket box cover on the International Space Station (ISS) after 1 year of space exposure.[10] In addition to causing AO undercutting, AO scattering can cause oxidation of sensitive components not normally in direct line-of-site with LEO AO, such as within a telescope body.

In order to design durable high-performance spacecraft systems, it is essential to understand the AO erosion yield (E_y) of materials being considered for spacecraft applications along with AO scattering characteristics. The E_y is the volume loss per incident oxygen atom (cm^3/atom). Materials spaceflight experiments for E_y determination have been flown on the Shuttle, the Long Duration Exposure Facility (LDEF), the Russian space station Mir and other spacecraft. More recently, they have been a part of the Materials International Space Station Experiment (MISSE) series flown on the exterior of the International Space Station (ISS). Scattering characteristics can include AO E_y of materials receiving scattered AO and information on the angular distribution of scattered AO, etc.

NASA Glenn Research Center developed an active flight experiment, called the Scattered Space Atomic Oxygen Experiment (SSAOE), to characterize AO scattering in space. The SSAOE was originally flown on the Wake Shield Facility (WSF) during the STS-60 shuttle mission, and was later flown as part of the MISSE 6 mission on the exterior of the ISS. This paper provides an overview of the SSAOE, information on the flight missions, and post-flight results on the angular distribution of LEO AO scattered off a 45° included fused silica slide. The LEO scattered AO erosion data can be used to improve AO undercutting models and improved the durability predictions of spacecraft components receiving scattered AO.

Scattered Space Atomic Oxygen Experiment (SSAOE)

Experiment Objectives and Design

The objectives of the SSAOE were to measure and compare direct ram AO erosion and scattered AO erosion in space, and to measure the angular distribution of AO scattered off an inclined angle. In addition, eight small passive samples were included on the space exposed surface to obtain ram AO erosion data on potential spacecraft materials. These objectives were to be achieved through three independent sub-experiments: 1). A two part **active experiment** to measure both in-situ direct ram AO erosion and in-situ scattered AO erosion within an active AO scatterometer, 2). A **passive AO scatterometer** to measure the angular distribution of LEO AO scattered off an inclined angle, and 3). **Passive samples** for directed LEO AO Ey characterization. A pre-flight photograph of the SSAOE is provided in Figure 4. A schematic drawing of the SSAOE is provided in Figure 5. This paper provides an overview of the SSAOE components, and provides post-flight photographs of the passive flight samples and detailed results from the passive AO scatterometer sub-experiment.

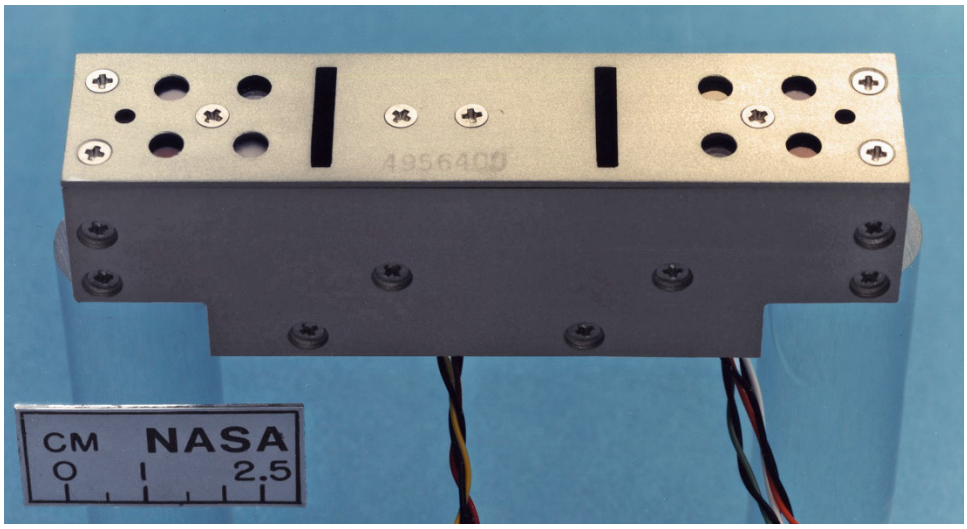

Figure 4. Pre-flight photograph of the SSAOE prior to the STS-60 flight.

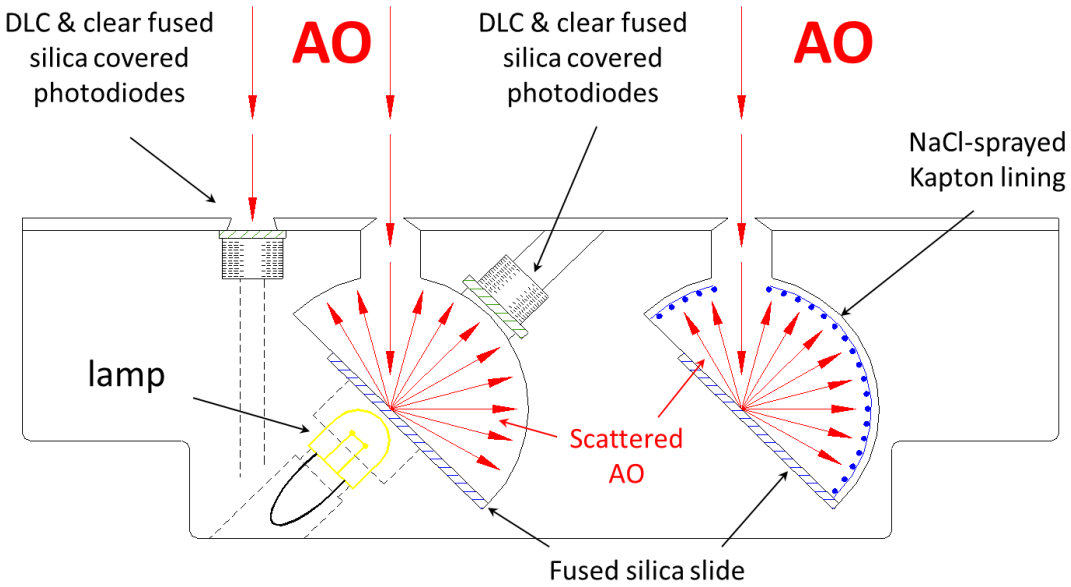

Figure 5. Schematic drawing of the SSAOE showing the active components, including the active scattering chamber (left) and the passive scattering chamber (right).

SSAOE Active Experiment

The SSAOE active experiment was designed to compare the in-situ erosion of opaque diamond-like carbon (DLC) exposed to direct ram LEO AO to the in-situ erosion of opaque DLC exposed to thermally accommodated scattered space AO. This was to be accomplished by measuring increases in light transmittance of small DLC coated fused silica samples as they became eroded by AO over-time in space. The increased transmittance would be measured through the use of photodiodes and two light sources. Each active sample had a corresponding control sample. The control sample was a clear fused silica slide over a second photodiode. For simplicity, both the DLC coated and clear fused silica samples were located in different sections of a single rectangular fused silica slide.

The direct ram LEO exposed active samples (DLC coated fused silica and clear fused silica) were located on the top, space exposed, surface of the SSAOE, as shown in Figure 5. The light source for the ram AO exposed sample (i.e., external) was the Sun. The active scattered AO experiment is set inside a cylindrical scatterometer where ram AO can enter the scatterometer chamber and scatter off a fused silica slide tilted at a 45° angle at the center of the chamber. The active AO scatterometer is the left chamber, as shown in Figure 5. The lamp, the clear fused silica slide (at a 45° angle) and the photodiode can be seen in the active AO scatterometer chamber. The light source for the scattered AO exposed sample was a GTE Sylvania Miniature Lamp (5.8 mm x 13.2 mm) Type 2187 (28 volts, 0.04 amps). The photodiodes, both external facing and inside the scatterometer, were Hamamatsu silicon photodiodes #S1226-18BD. These photodiodes have 1.1 mm x 1.1 mm photo-sensitive areas with a spectral response range of 190-1000 nm and a peak wavelength at 720 nm.

Figure 6 provides a pre-flight photograph of the SSAOE with one side removed. This image shows the shape of the two scatterometer chambers (passive chamber on the left and active chamber on the right). Figure 7 provides a pre-flight photograph of the SSAOE with the active experiment components exposed and labeled. Table 1 provides a list of the active experiment materials. Figure 8 provides a pre-flight photograph of the SSAOE showing the internal DLC coated and clear fused silica samples sitting over photodiodes. In addition, the active AO scatterometer chamber was lined with microscopically textured Kapton (AO textured) on both side-walls, and along the cylindrical area, as seen in Figures 6 and 8, as an oxygen “getter” to reduce subsequent AO scattering.

SSAOE Passive AO Scatterometer

The SSAOE passive scatterometer chamber can be seen on the right in the schematic drawing in Figure 5 and on the left in the photographs in Figures 6-8. Like the active chamber, the passive scatterometer chamber allows ram AO to enter the chamber and scatter off a fused silica slide tilted at a 45° angle at the center of the chamber. The cylindrical section of the passive chamber was lined with a salt-sprayed Kapton H sample so that the angular distribution of scattered AO can be determined post-flight based on erosion depth (recession depth) measurements after the salt is washed off post-flight. Thus, the passive scatterometer will provide information on the degree of specular scattering of AO. This salt-sprayed Kapton H liner is identified in Figure 5 and can be seen in Figure 8. The passive AO scatterometer chamber was also lined with microscopically textured Kapton (AO textured) on both side-walls. Figure 9 provides a pre-flight photograph of the SSAOE showing the textured Kapton side walls on one side of the active and passive scatterometer chambers.

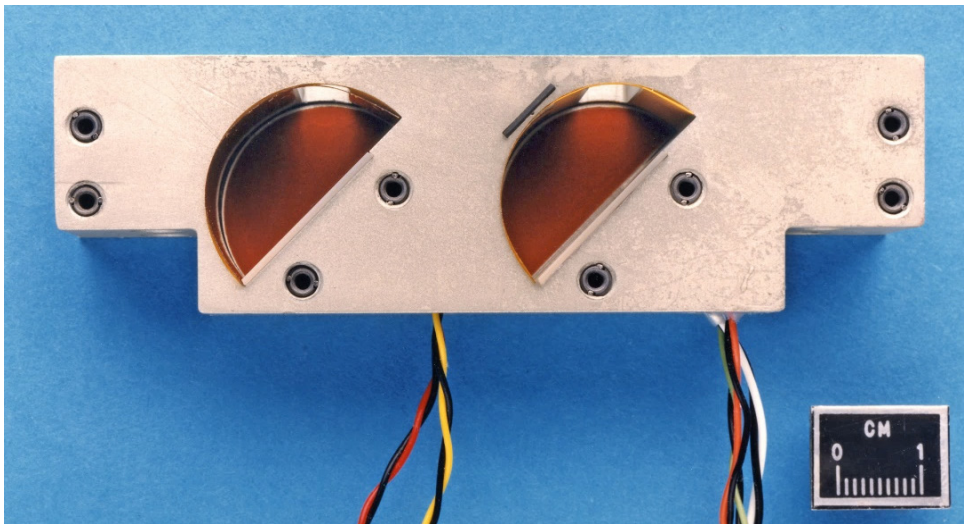

Figure 6. Pre-flight photograph of the SSAOE with one side removed showing the two scatterometer chambers (passive on the left and active on the right).

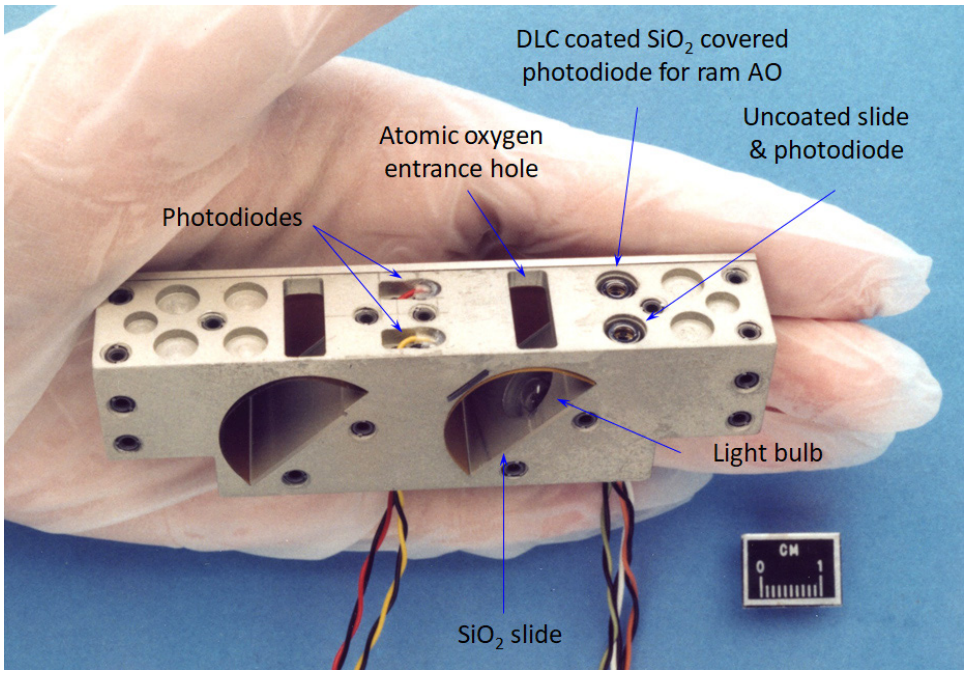

Figure 7. Pre-flight photograph of the SSAOE with the active components labeled.

Table 1. MISSE 6 SSAOE Active Experiment Materials

Sample ID	Material	Location	Notes
A1	1/2 DLC coated & 1/2 clear fused silica slide	Slide covering ram facing photodiodes	DLC coated area is the test area, clear fused silica area provides light calibration
A2	1/2 DLC coated & 1/2 clear fused silica slide	Slide covering internal scatterometer photodiodes	DLC coated area is the test area, clear fused silica area provides light calibration
A3	Fused silica slide	45º angled slide in center of scatterometer (covering lamp)	Provides scattered AO to internal samples
A4	Salt-sprayed Kapton H	Passive scatterometer cylindrical lining	For determining angular dependence on Ey
A5	Textured Kapton H	Scatterometer wall linings	Acts as an AO getter to minimize scattered AO

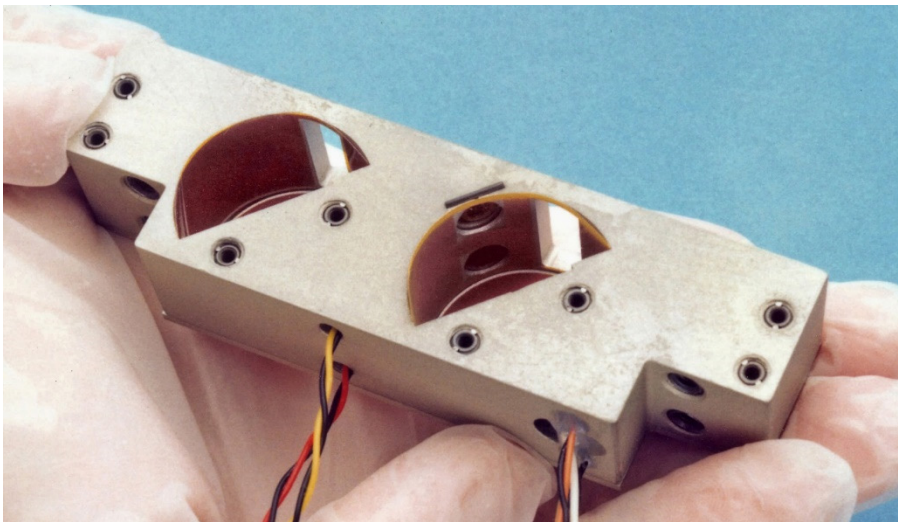

Figure 8. Pre-flight photograph of the SSAOE showing the internal DLC coated fused silica samples in the active AO scatterometer chamber (right) and Kapton AO getter lining.

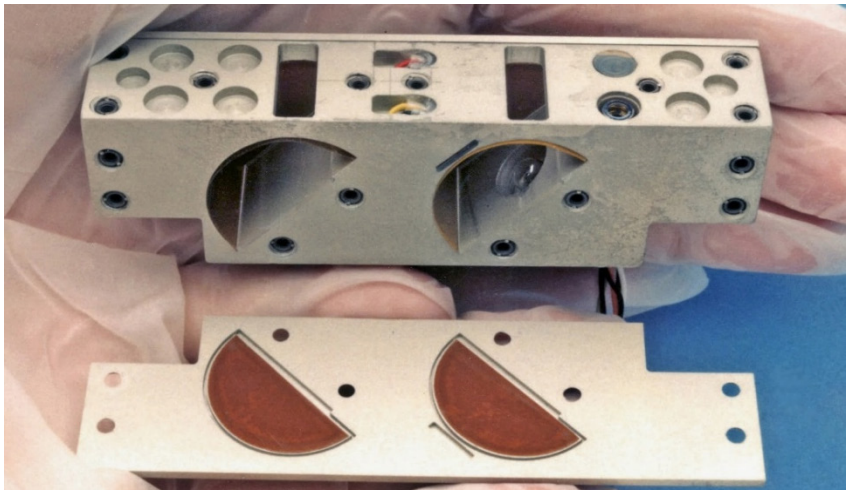

Figure 9. Pre-flight photograph of the SSAOE showing the two textured Kapton side walls on one side of the active and passive scatterometer chambers.

SSAOE Passive Samples

Eight small passive samples were included on the top (i.e., ram facing) surface of the SSAOE so that ram AO E_y data could be obtained on passive flight samples. These samples are listed in Table 2 and the locations of the samples are shown in the post-flight photograph in Figure 10. Six of the passive samples were 0.25-inch diameter and two samples were 0.09-inch diameter. Because of the small size, six of the samples were salt-sprayed pre-flight so that recession depth measurements could be made post-flight because this technique works well for small samples and low AO fluence exposures.[11,12] Because the carborane-siloxane (P1) and CV1144 coated Kapton (P6) samples are Si based samples, they were not salt-sprayed. These samples are not expected to erode, because they will convert to a glassy layer with AO exposure. The Kapton HN sample (P8) was flown with two stacked layers: a salt-sprayed 2 mil top layer and a 5 mil (non-salt-sprayed) bottom layer. The full MISSE 6 flight sample IDs for these samples are G3-SSAOE-P#.

Table 2. SSAOE Passive AO Erosion Samples

SSAOE ID	Material	Salt-Sprayed	Size (area)
P1	Carborane-Siloxane	No	0.25” dia. (0.05 in.^{2})
P2	Teflon AF-1600	Yes	0.25” dia. (0.05 in.^{2})
P3	Teflon FEP	Yes	0.25” dia. (0.05 in.^{2})
P4	Epoxy-silane (HRG-3/AO)	Yes	0.09” dia. (0.006 in.^{2})
P5	Epoxy-silane (HRG-3/AB)	Yes	0.09” dia. (0.006 in.^{2})
P6	CV1144 coated Kapton	No	0.25” dia. (0.05 in.^{2})
P7	Polyphosphazene	Yes	0.25” dia. (0.05 in.^{2})
P8	Kapton HN (2 mil layer/5 mil layer)	Yes (2 mil top layer)	0.25” dia. (0.05 in.^{2})

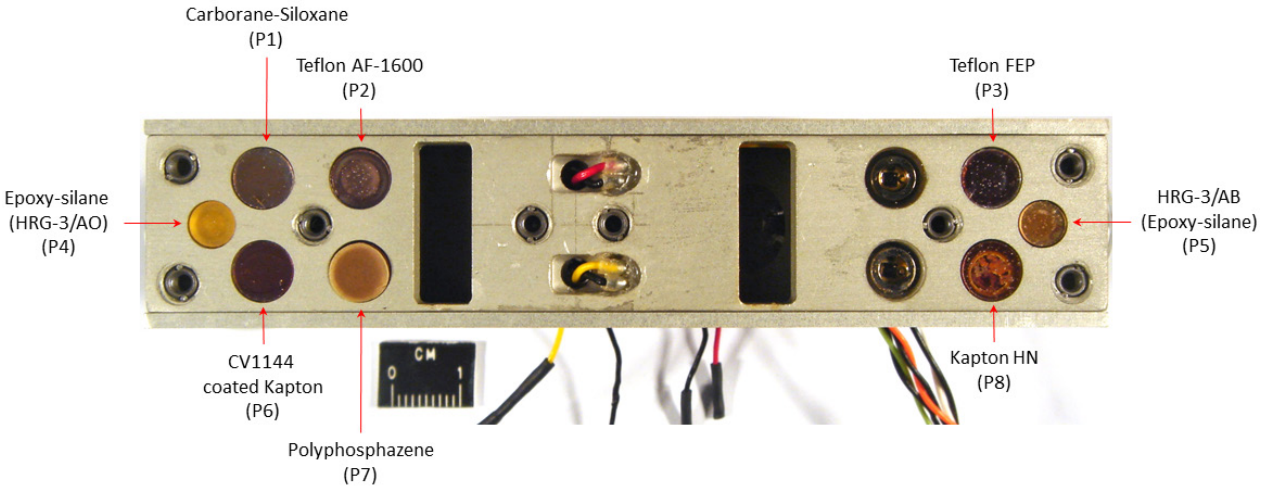

Figure 10. Post-flight photograph of the SSAOE with the lid removed and the eight passive AO samples labeled.

Flight Missions

STS-60 Wake Shield Facility (WSF)

The SSAOE was originally flown as part of the Materials Laboratory Experiment-1, also called the Materials Laboratory-1 (MatLab-1). The MatLab-1 was conducted with the Materials Flight Experiment (MFLEX) carrier mounted on the front (ram side) of the Wake Shield Facility (WSF) during the STS-60 shuttle mission, which occurred February 3-11, 1994.[13] Due to complications during the mission, the SSAOE and other active MatLab-1 experiments were exposed to ram AO on the front side of the WSF for only 40-45 hours while the WSF was attached to the shuttle's remote manipulator arm, as shown in Figure 11a.[13] Figure 11b provides a close-up photograph of the MatLab-1 on the front of the WSF during STS-60 with the SSAOE out-lined in red.

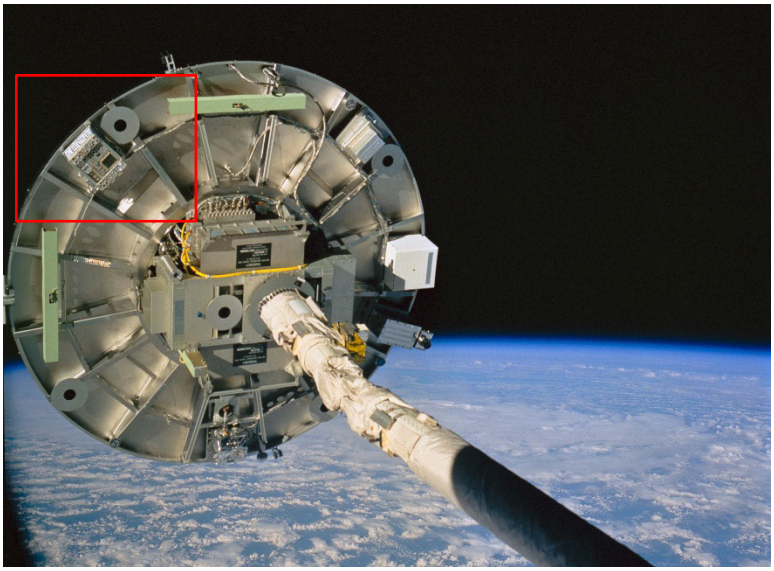

a.

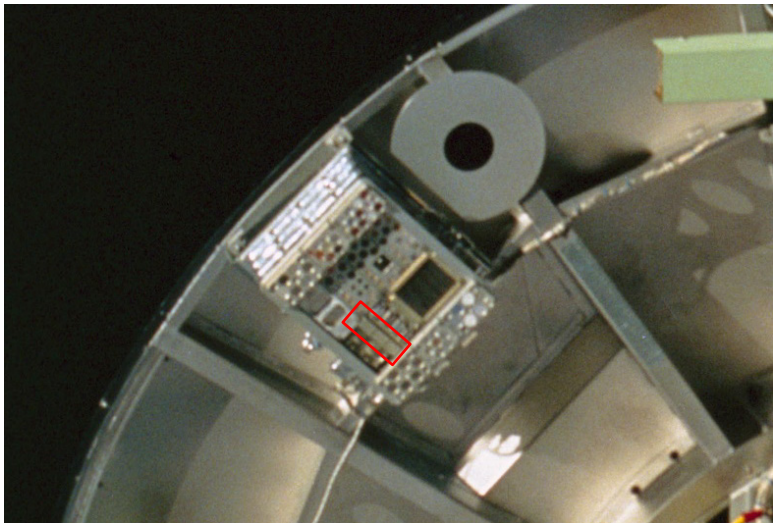

b.

Figure 11. Photographs of the WSF during the STS-60 mission: (a). The WSF on the shuttle's remote manipulator arm, and (b). Close-up photograph (red boxed area in Figure 11a) of the MatLab-1 with the SSAOE outlined in red.

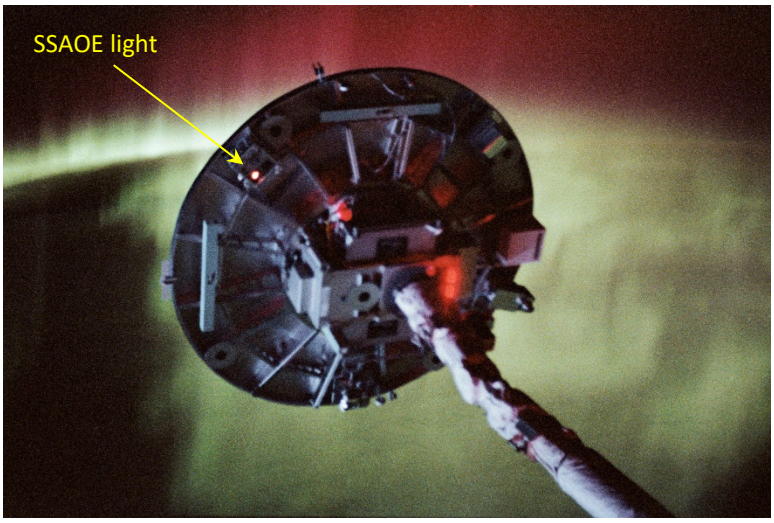

Figure 12. Night time photograph of the WSF with aurora during the STS-60 mission. The small bright glow from the SSAOE lamp can be seen in the upper-left area of the WSF.

It was estimated that the active samples on the MatLab-1 were exposed to an AO fluence of only 3.5 x 10^{19} atoms/cm^2 during the mission.[13] Although the SSAOE was active during the exposure, as witnessed by the light seen in the night time photograph shown in Figure 12, the AO fluence for the mission was too low to obtain meaningful active data. Therefore, it was decided to re-fly the SSAOE as part of one of the MISSE missions. Therefore, the SSAOE, including all active and passive samples was re-flown as part of the MISSE 6 mission.

Materials International Space Station Experiment 6 (MISSE 6)

The Materials International Space Station Experiment (MISSE) program involves a series of spaceflight missions with experiments flown on the exterior of the ISS to test the performance and durability of materials and devices exposed to the LEO space environment. In the MISSE 1–8 missions, individual flight experiments were flown in suitcase-like containers called Passive Experiment Containers (PECs) that provided exposure to the space environment. The PECs were placed outside the ISS in various locations by an astronaut during an extravehicular activity (EVA), or spacewalk. The PECs were positioned in either a ram/wake or a zenith/nadir orientation, and exposed for 1-4 years between August 2001 and July 2013.

The SSAOE was located on the ram side of MISSE PEC 6B in the G3 Tray. MISSE PEC 6A and 6B were installed on the exterior of the ISS Columbus Laboratory and deployed on March 22, 2008 during the STS-123 shuttle mission. Both MISSE 6A and 6B were oriented in ram/wake orientations so that the ram surfaces would receive directed ram AO exposure during the majority of the mission. The MISSE 6A and 6B PECs received approximately 1.45 years of space exposure, until they were retrieved on September 1, 2009 during the STS-128 shuttle mission. Figure 13 shows the MISSE 6A and 6B on the exterior of the Columbus Laboratory in March 2008 during the STS-123 mission. Figure 14 is a close-up of MISSE 6A and 6B with the location of the SSAOE indicated.

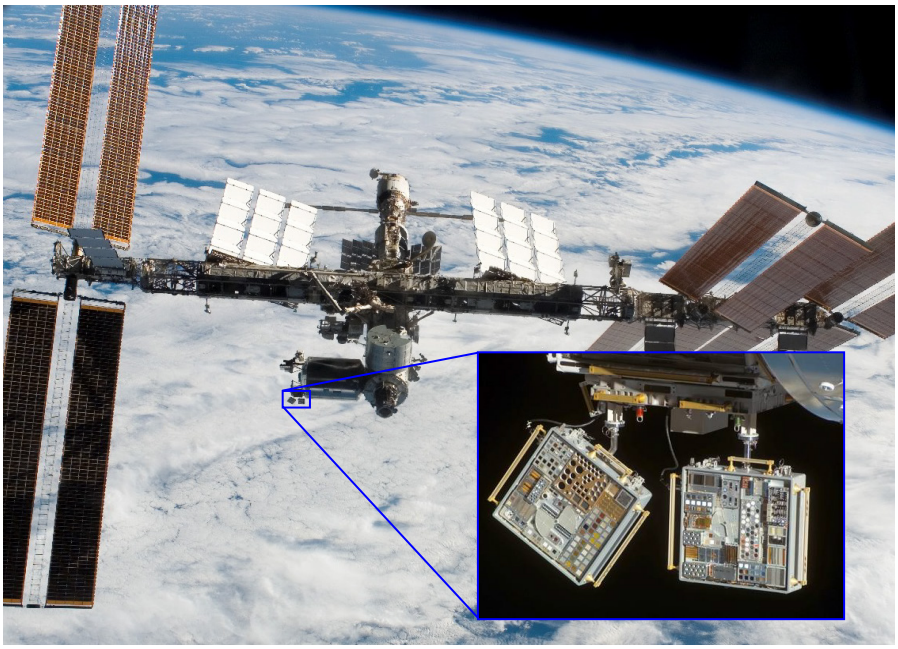

Figure 13. The ISS with a close-up photo of MISSE 6A (left) and 6B (right) on the Columbus Laboratory in March 2008.[9]

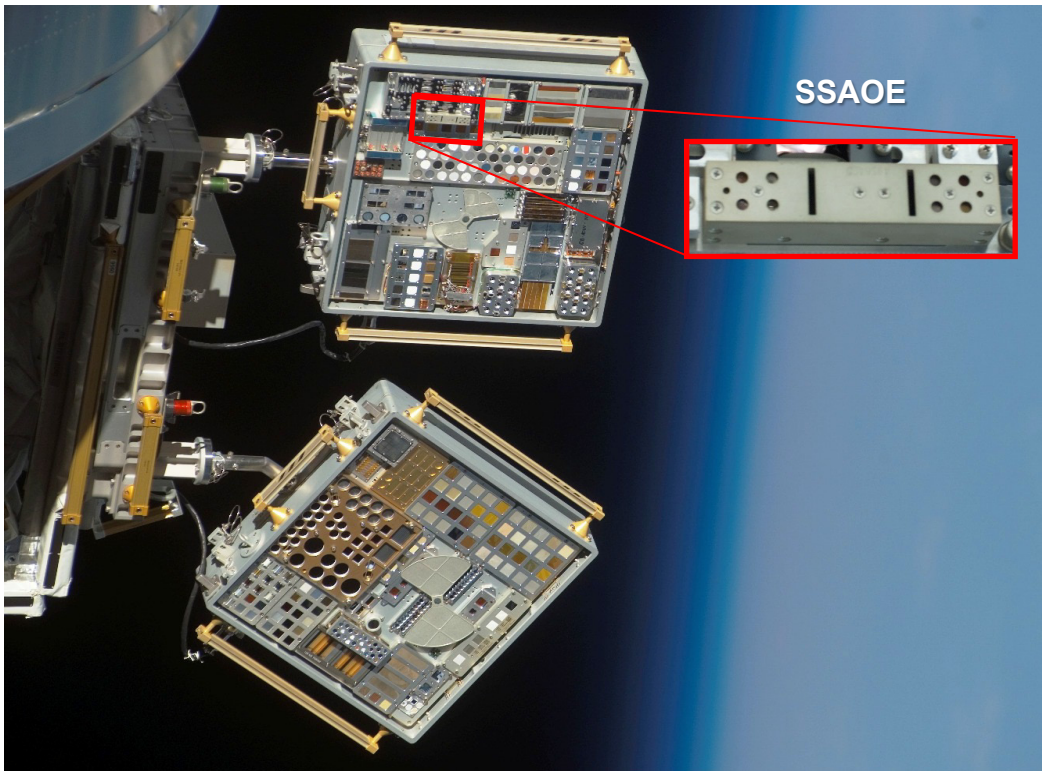

Figure 14. MISSE 6A (bottom) and MISSE 6B (top) on the Columbus Laboratory showing the location of the SSAOE on MISSE 6B with a close-up on-orbit image of the SSAOE.

Unfortunately, it was determined post-flight that the 15 volt power supply was not available to the SSAOE during the MISSE 6 mission, so the lamp and photodiodes did not operate on-orbit as planned. Therefore, SSAOE active experiment data is not available from the MISSE 6 mission. Only data from the passive sub-experiments could be analyzed post-flight.

The MISSE 6B ram AO fluence was based on the mass loss of a Kapton H witness sample (W6-5) flown in the W6 tray on the ram side of MISSE 6B.[14] The MISSE 6B ram fluence was determined to be $1.90 \pm 0.05 \times 10^{21}$ atoms/cm^2.[14] Estimates of solar exposures for the MISSE 6 trays were obtained using the Boeing Integrated ISS TRASYS model for solar exposure levels for the surface of the Columbus module near the location of MISSE 6. The solar exposure for the MISSE 6 ram surfaces was estimated at 2,600 equivalent sun hours (ESH).[15]

Post-Flight Experimental Procedures

Field Emission Scanning Electron Microscope (FESEM)

Scanning electron microscope (SEM) images were obtained using Hitachi S-4700 field emission scanning electron microscope (FESEM) operated at an accelerating voltage from 1-3 kV, but typically at 3 kV. The sample was coated with a thin conductive layer (Pt-Pd) so it would not charge during SEM imaging. Images were taken at magnifications from 9kX to 35kX.

Erosion Depth Measurements

The erosion depth, or recession depth, of the salt-sprayed Kapton scatter chamber liner was determined using SEM imagery at 15° scatter angles. The scatter angle is the angle at which the incoming AO was scattered off the fused silica slide positioned at 45° in the center of the scatter chamber, as shown in Figure 15. It should be noted that the "scatter angle" is different than the "sample angle." The samples angle is also included in Figure 15 in red. Images were taken of the erosion step-heights (i.e., erosion depth) after the salt particles were gently washed off with distilled water. The sample was then coated with a thin Pt-Pd conductive layer for SEM imaging. The SEM images were taken with the sample surface at a 45° tilt angle (θ) to the electron beam.

Between 3 and 17 images were taken of the Kapton lining at each scatter angle, and of these, between 1 and 11 images were selected for erosion depth measurements. Then, between 1 and 3 salt-protected sites best suited (i.e., greatest depth location) for obtaining height measurements were located on each image. The erosion depth for each scatter angle was determined by measuring the difference in height (i.e., depth) of the salt-protected and non-protected area of an enlarged print (8.5" x 11") of the sample image with a digital caliper at each of the selected locations.

The SEM image erosion depth (d) measurements, obtained at a 45° tilt angle, were used to compute the actual depth of erosion. The actual erosion depth (D) was determined from the SEM measured depth by correcting for the 45° angle imaging perspective as shown in Figure 16, where e^- is the electron beam and $D = d/\sin\theta$. The actual erosion depth values were used to compute the average erosion depth for each scatter angle as well as the standard deviation.

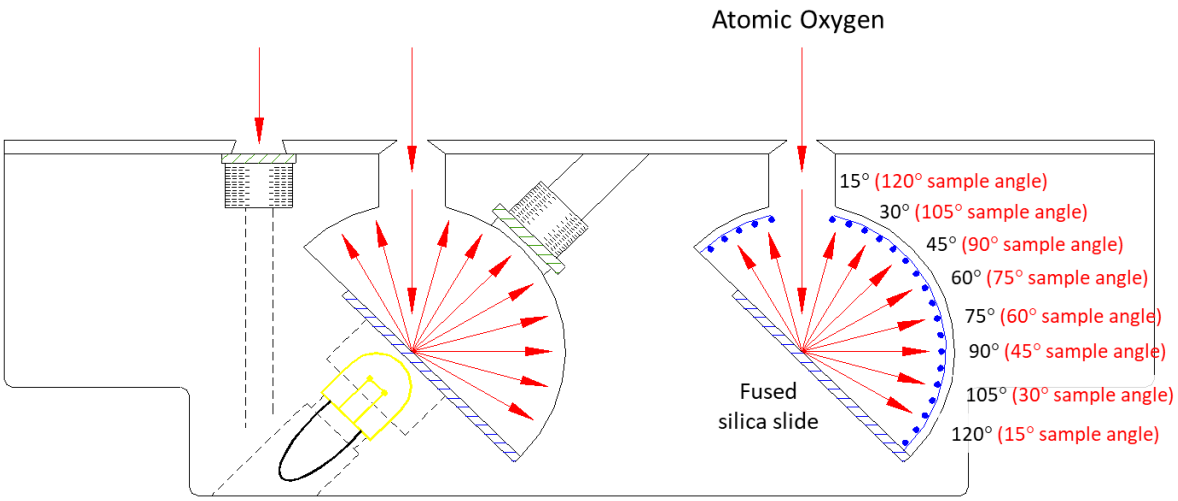

Figure 15. SSAOE passive scattering chamber with the scatter angles provided in black and the sample angles provided in red.

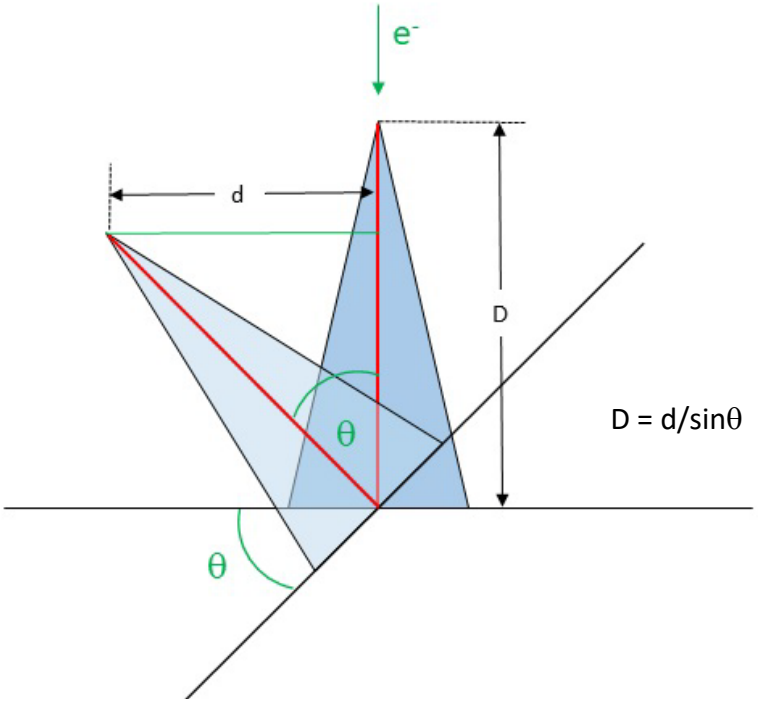

Figure 16. Schematic image showing the actual erosion depth (D) and SEM erosion depth (d) as imaged at an θ angle (45°) in the SEM.

It should be noted that when a sample is eroded by directed ram AO in LEO, microscopic "erosion cones" develop as part of the erosion process for materials with volatile oxidation products. These cones provide microscopic texture. Schematic images of the texture is provided in Figures 17a and 17b. As can be seen in Figure 17a, the actual erosion depth (D) is from the center of the microscopic cone texture (A) to the top of the protected surface, or butte. Figure 17b shows the actual dimensions (H, D, A) and those imaged and measured at an SEM tilt angle θ (h, d, a).

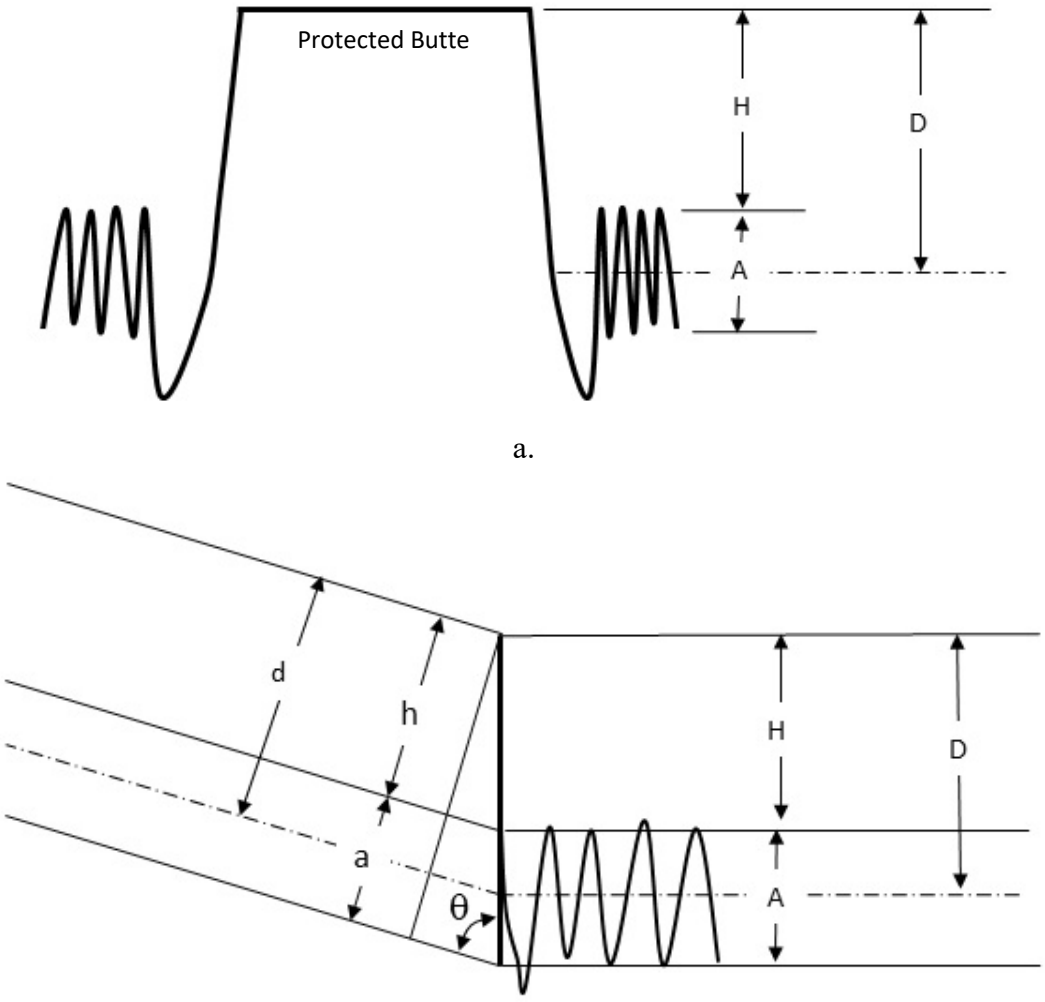

Figure 17. Schematic illustrations of a protected butte and corresponding AO erosion texture (A): (a) Protected butte with height to the top if the erosion texture (H), the height of the erosion texture (A) and the actual erosion depth (D), and (b) Actual erosion texture dimensions (H, D and A) and those imaged and measured at an SEM tilt angle θ (h, d, a).

Equations 1-5 show that the actual erosion depth (D) is simply equal to the SEM measured depth (d) divided by the sin of the SEM tilt angle (θ).

$$D = H + A/2 \quad \text{Equation 1}$$

$$H = h/sin\theta \quad \text{Equation 2}$$

$$A = a/sin\theta \quad \text{Equation 3}$$

$$\text{Thus, } D = h/sin\,\theta + a/(2sin\theta) \quad \text{Equation 4}$$

$$\text{Or simply, } D = d/sin\theta \quad \text{Equation 5}$$

The actual erosion height (D) was used to compute the E_y at a specific scatter angle using Equation 6:

$$E_y = \frac{D}{F} \quad \text{Equation 6}$$

E_y = Erosion yield (cm^3/atom)
D = Actual erosion depth (cm)
F = Atomic oxygen fluence (atoms/cm^2)

Results and Discussion

Figure 18 provides a post-flight photograph of the SSAOE after the MISSE 6 mission. Figure 19 shows a post-flight photograph of the SSAOE with the lid removed and the small passive samples and the ram facing photodiodes visible.

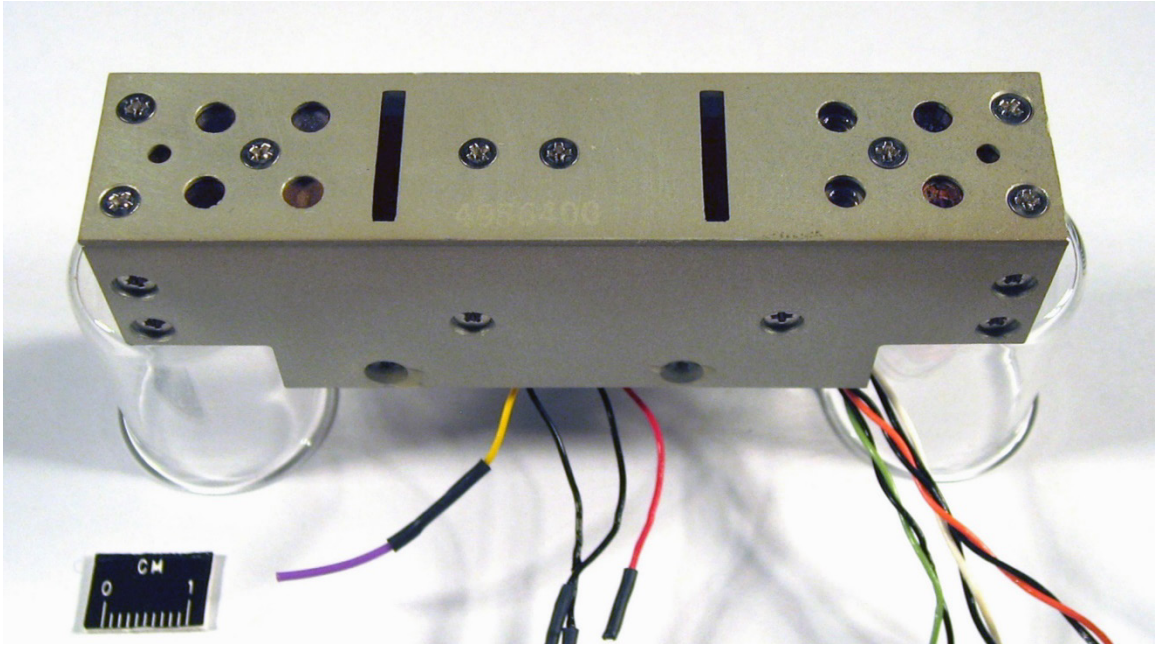

Figure 18. Post-flight photo of the SSAOE after the MISSE 6 mission.

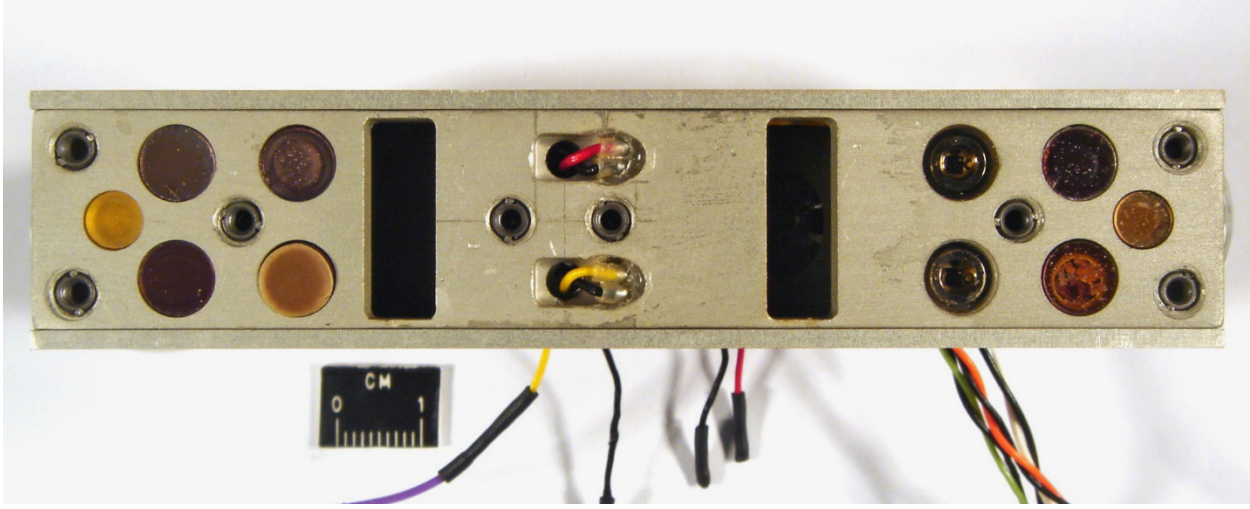

Figure 19. Post-flight photograph with the lid removed and the passive samples and ram facing photodiodes visible.

Passive Samples

Figures 20a-20h provide post-flight photographs of the ram facing passive flight samples along with corresponding control samples. The flight sample is on the left and the control sample is on the right in each photograph. As can be seen, several samples have darkened due to space exposure. This includes significant darkening of P1 (carborane-siloxane), P2 (Teflon AF-1600), P5 (Epoxy-silane (HRG-3/AB)) and P7 (polyphosphazene), as shown in Figures 20a, 20b, 20e, and 20g, respectively. Sample P4 (Epoxy-silane (HRG-3/AO)) darkened a little, as shown in Figure 20d. The Teflon FEP sample (P3) did not discolor, as shown in Figure 20c. And, the CV1144 coated Kapton (P6) does not appear to have darkened, although it is difficult to tell since the sample was dark to start with. Sample P7 (polyphosphazene) became embrittled due to space exposure and has cracked. It should be noted that the polyphosphazene control sample is now very curled, as shown in Figure 20g. And, as can be seen in Figure 20h, the top 2 mil layer of the Kapton HN sample (P8) was eroded completely through in the majority of the exposed area and the underlying 5 mil thick Kapton HN layer was partially eroded in the locations where the top 2 mil layer was gone.

The LEO E_y for Kapton HN has been determined to be 2.81×10^{-24} based on the NASA Glenn MISSE 2 Polymers Experiment that was exposed to LEO ram AO for four years.[2] Thus, a rough estimate of the AO fluence for the SSAOE experiment can be determined based on the observed erosion of the top 2 mil layer (0.00508 cm) of the P8 Kapton HN sample. Using the MISSE 2 E_y for Kapton HN, the AO fluence for the SSAOE passive samples is estimated at 1.81×10^{21} atoms/cm^2. This fluence is close to the more accurately determined AO fluence for the MISSE 6 mission using a larger Kapton H AO fluence sample (W6-5) and based on pre- and post-flight dehydrated mass measurements, which provided a mission fluence of $1.90 \pm 0.005 \times 10^{21}$ atoms/cm^2. Recession based E_y values for these passive ram samples are not included in this report. But, as can be seen in the post-flight photographs all samples survived the 1.90×10^{21} atoms/cm^2 AO fluence with color changes as the most significant degradation.

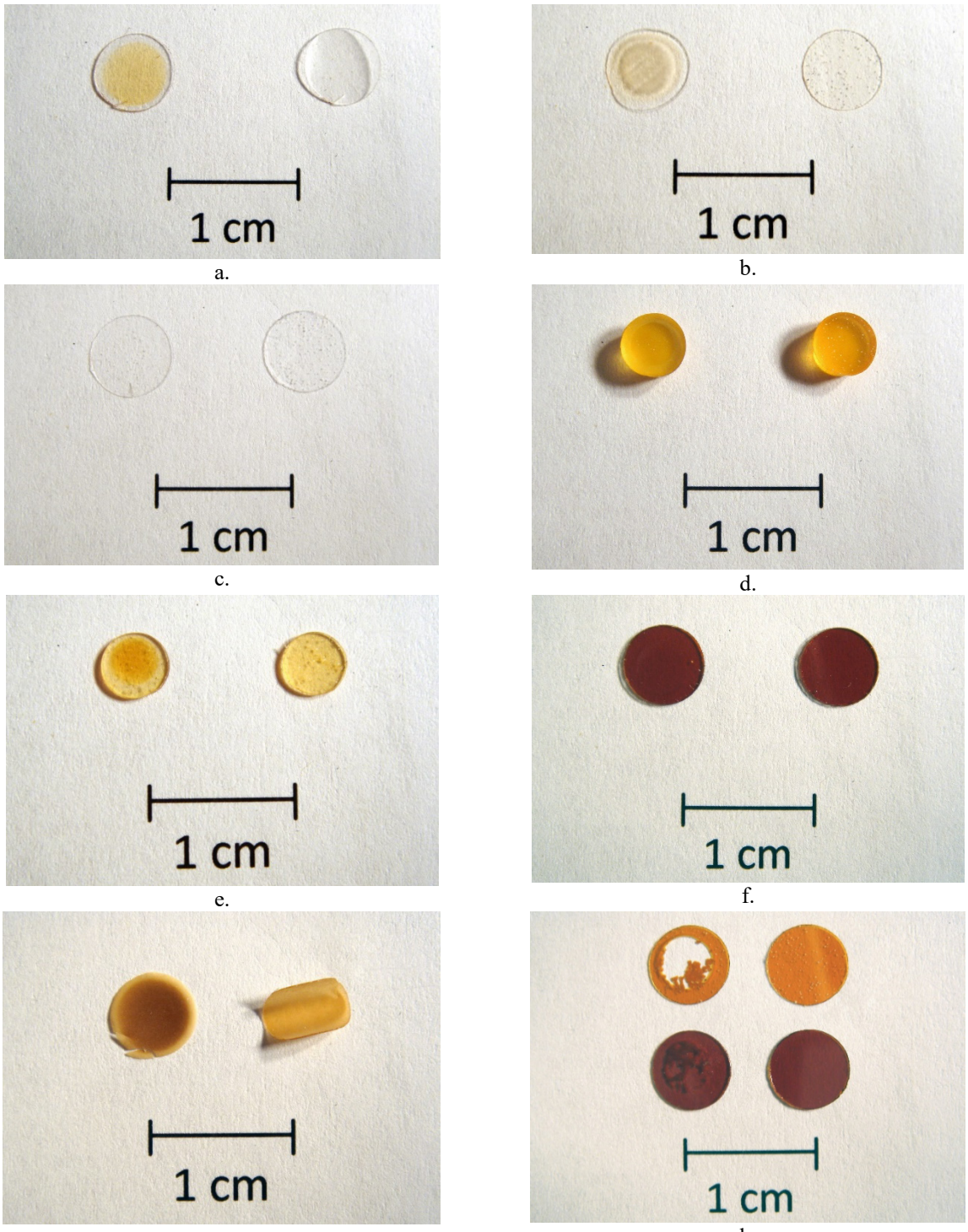

Figure 20. Post-flight photographs of the passive ram flight samples (left) and control samples (right): (a) P1 (carborane-siloxane), (b) P2 (Teflon AF-1600), (c) P3, (d) P4 (epoxy-silane (HRG-3/AO)), (e) P5 (epoxy-silane (HRG-3/AB)), (f) P6 (CV1144 coated Kapton), (g) P7 (polyphosphazene), and h). P8 (Kapton HN) with the space exposed 2 mil top layer in the upper left and the underlying 5 mil flight samples on the bottom left.

SSAOE Passive AO Scatterometer

Figure 21 and Figure 22 provide post-flight photographs with one of the SSAOE sides removed. Figure 21 shows the inside of both the active (right) and passive (left) scatterometer chambers and Figure 22 is a close-up of the passive scatterometer chamber showing the salt particles remaining on the Kapton liner. Figure 23 shows the passive scatterometer salt-sprayed Kapton liner removed from the scatterometer chamber and Figure 24 shows passive scatterometer salt-sprayed Kapton liner sample sectioned, and prepared for SEM imaging.

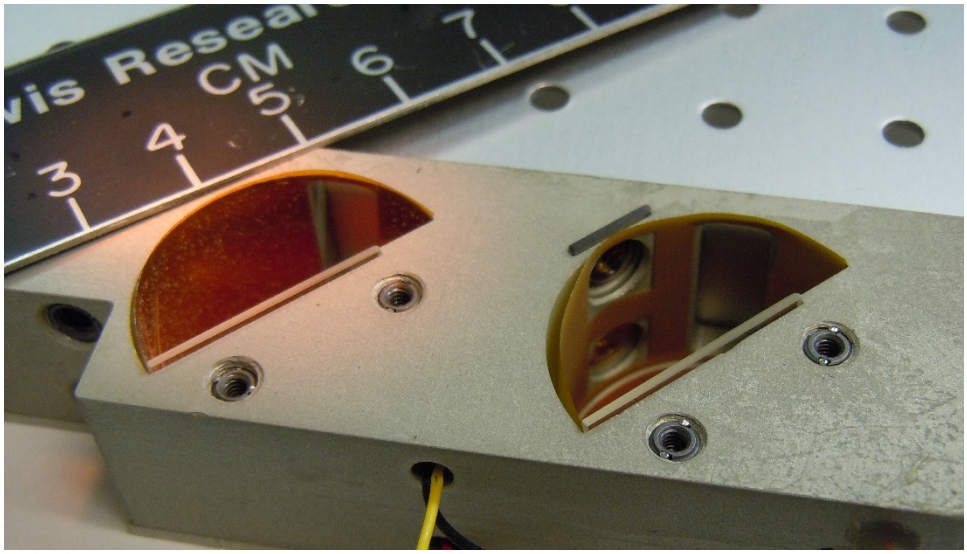

Figure 21. Post-flight photograph showing the inside of both the active (right) and passive (left) scatterometer chambers.

Figure 22. Post-flight photograph of the passive scatterometer chamber showing salt remaining on the Kapton liner.

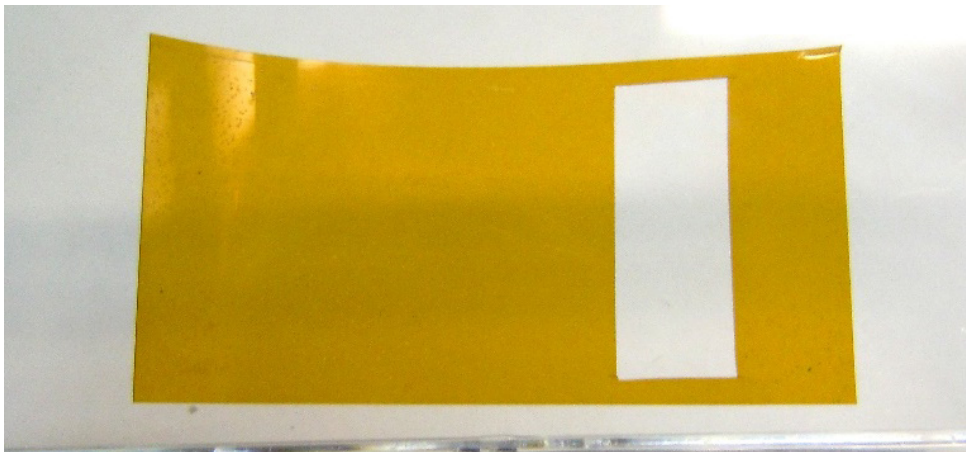

Figure 23. Post-flight photograph of the passive scatterometer salt-sprayed Kapton liner.

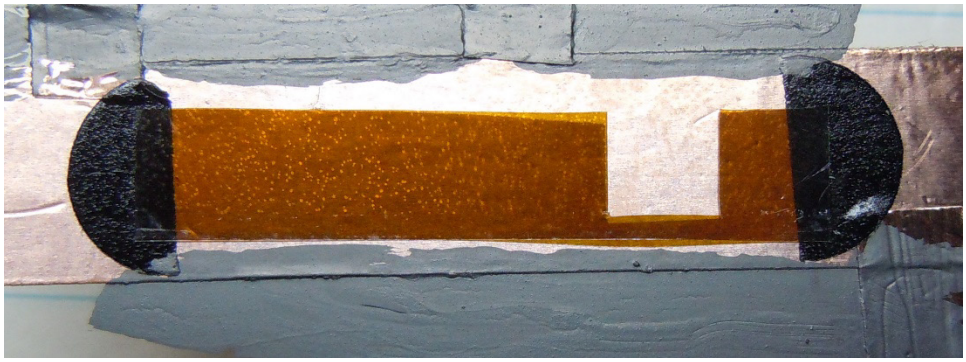

Figure 24. Post-flight photograph of the sectioned passive scatterometer salt-sprayed Kapton liner sample prepared for SEM imaging.

Figure 25 is a SEM composite image, made up of many SEM images, showing the passive scatterometer Kapton liner with the salt-particles intact with the scatter angle locations defined. Figure 25a shows the **sample angles** and Figure 25b shows the **scatter angles**. As stated previously, the "sample angle" is not the same as the "scatter angle". The 15° sample angle is for the 120° scatter angle, the 30° sample angle is for the 105° scatter angle, the 45° sample angle is for the 90° scatter angle, the 60° sample angle is for the 75° scatter angle, the 75° sample angle is for the 60° scatter angle, the 90° sample angle is for the 45° scatter angle, and the 120° sample angle is for the 15° scatter angle. This is clarified to avoid confusion because the **sample angles** are listed on the SEM images (i.e., SSAOE15). SEM images were obtained at each angle shown in Figure 25 except at a 105° scatter angle (30° sample angle). Figure 26 provides SEM images of the passive scatterometer salt-sprayed Kapton liner with the salt particles present. As can be seen, the salt particles appears to have dried formed in clusters.

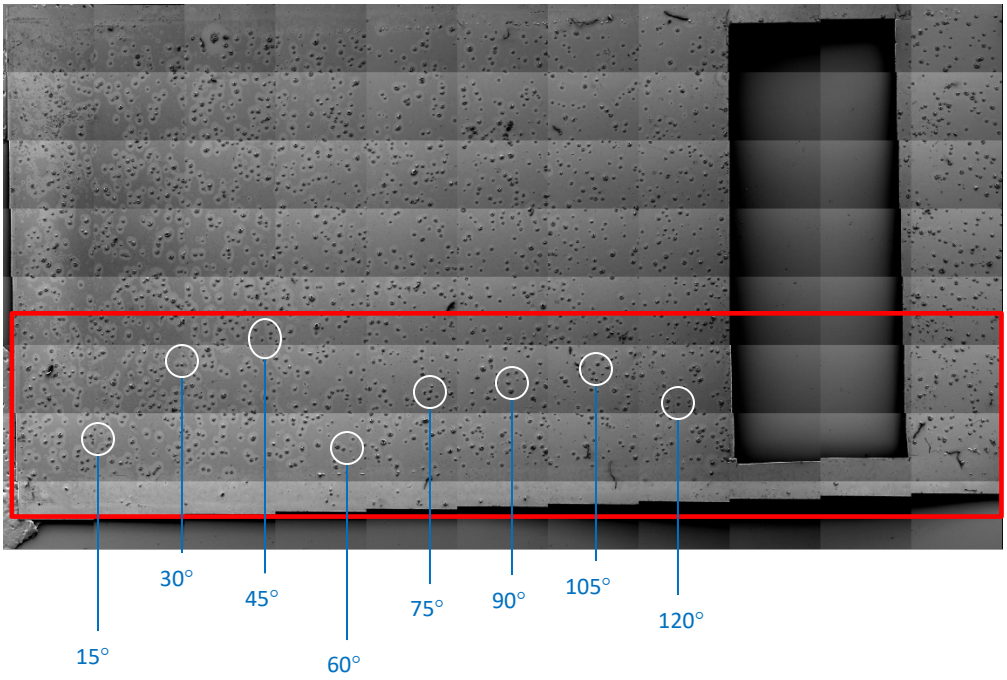

a.

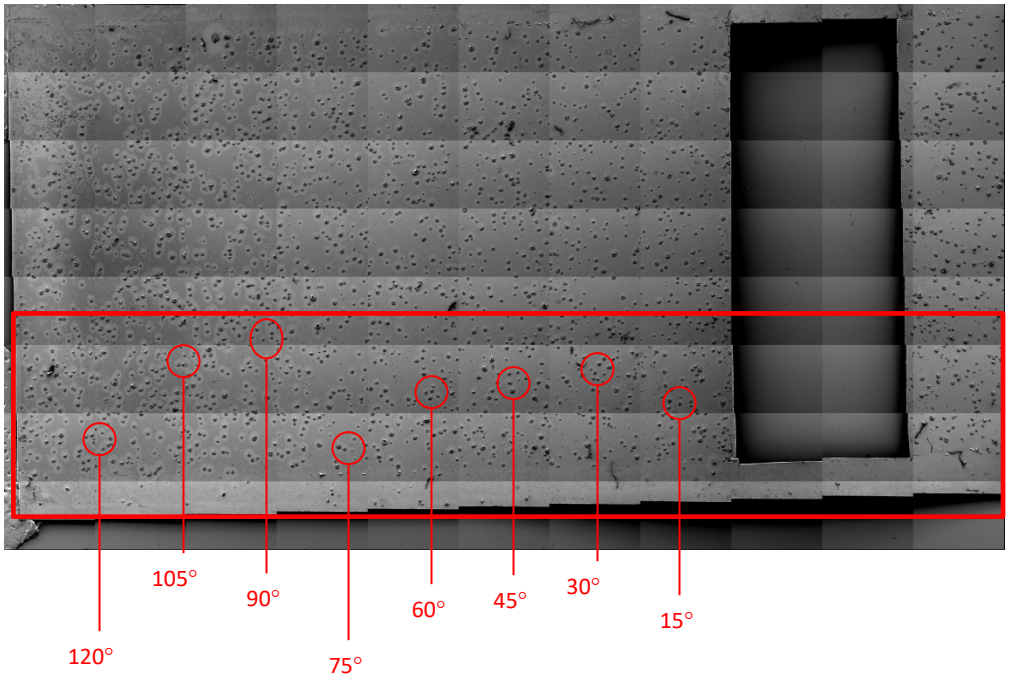

b.

Figure 25. SEM composite image of the passive scatterometer salt-sprayed Kapton liner with sample and scatter angles highlighted for the FESEM images: (a) Sample angles (blue), and (b) Scatter angles (red).

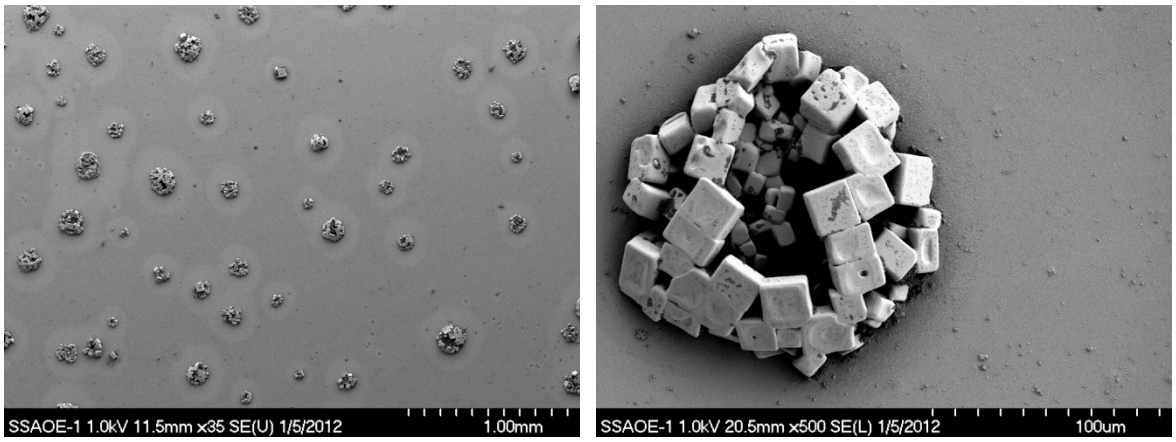

a. b.

Figure 26. SEM image pf the passive scatterometer salt-sprayed Kapton liner with the salt particles (i.e., clusters): (a) Lower magnification (imaged at 35X) image showing numerous salt clusters, and (b) Higher magnification (images at 500X) showing a single salt cluster.

Figures 27 to 34 provide examples of the SEM images used to obtain erosion depth (d) measurements. All the images were taken after the salt particles were washed off and at a 45° tilt angle. The erosion depth (d) was measured from the top of the salt-protected butte to the center of the erosion texture. An example of the measured height, d, is provided in Figure 27. It should be noted that selection of the best location to measure the erosion depth is objective and thus can introduce error into the measurements.

Figure 28 provides images taken at a 15° sample angle, which is a 120° scatter angle. Figure 29 provides images taken at a 30° sample angle, which is a 105° scatter angle. Figure 30 provides images taken at a 45° sample angle, which is a 90° scatter angle. Figure 31 provide images taken at a 60° sample angle, which is a 75° scatter angle. Figure 31b shows that there is not a clean step-height region due to the “double step”. Thus, measurements were not made at the 60° sample angle as the SEM butte images were not appropriate for good depth measurements. Figure 32 provides an image taken at a 75° sample angle, which is a 60° scatter angle. Figure 33 provides images taken at a 90° sample angle, which is a 45° scatter angle. No SEM images, and hence no erosion depth measurements were taken at a 105° sample angle (30° scatter angle). And, finally, Figure 34 provides an image taken at a 120° sample angle, which is a 15° scatter angle.

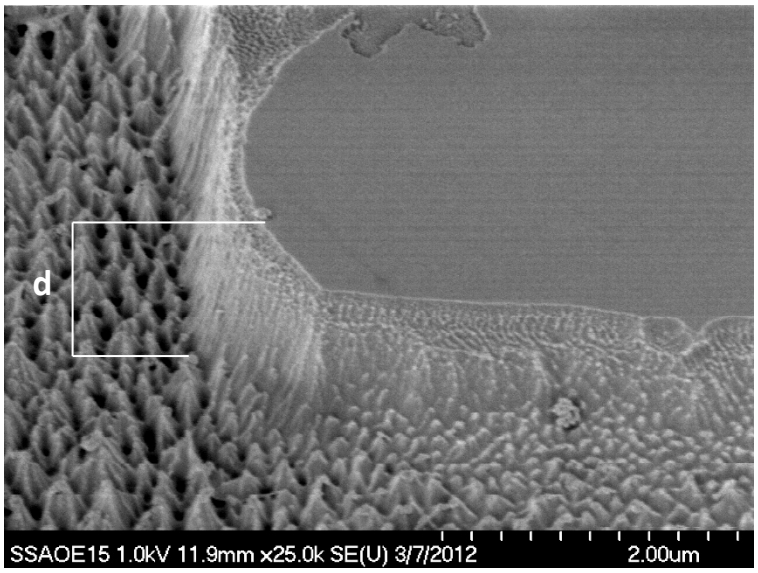

Figure 27. SEM image (SSAOE-15-45_08) at a sample angle of 15° (scatter angle of 120°) and at a 45° SEM title angle with the erosion depth (d) measurement location indicated.

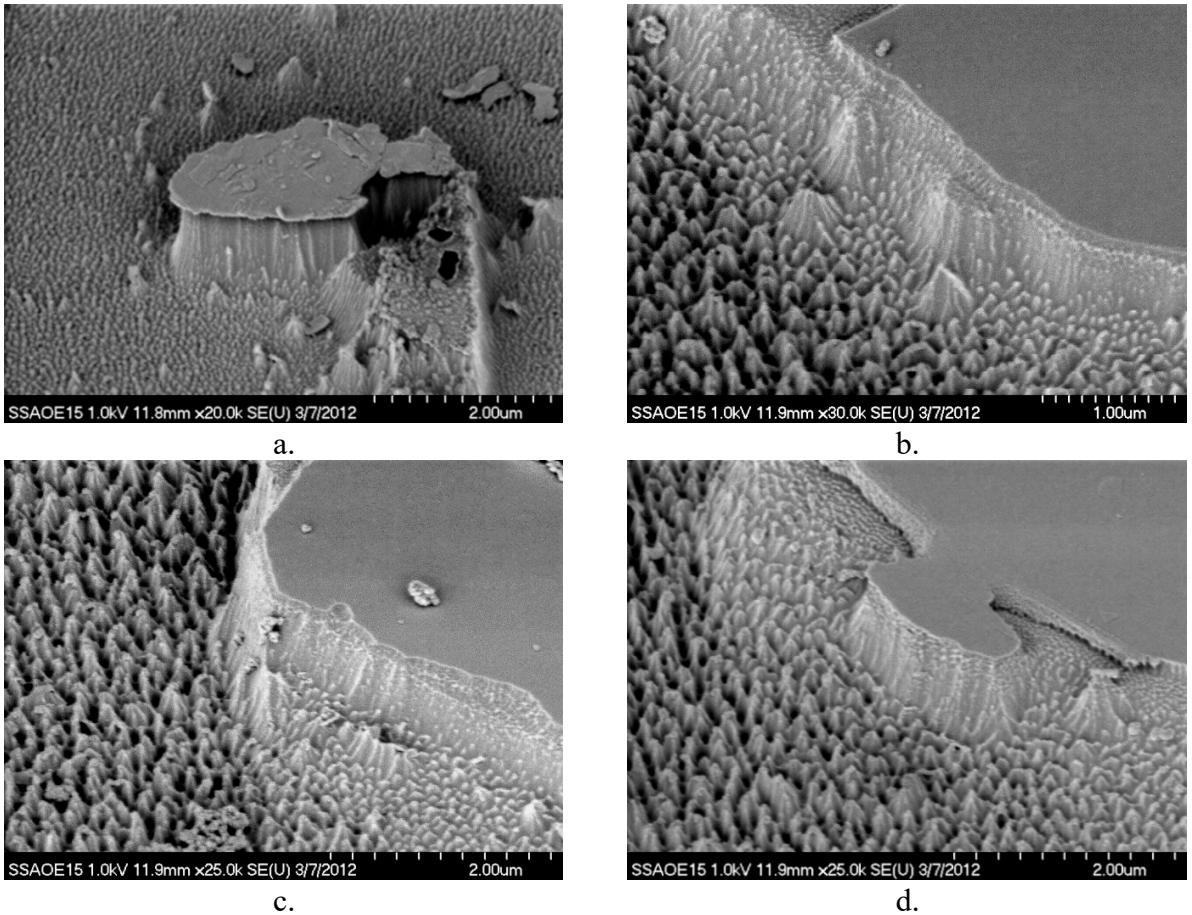

a. b. c. d.

Figure 28. SEM images of salt protected buttes taken at the 15° sample angle (120° scatter angle) and at a 45° SEM title angle: (a) Image SSAOE-15-45_02 taken at 20kX, (b) Image SSAOE-15-45_04 taken at 30kX, (c) Image SSAOE-15-45_06 taken at 25kX, and (d) SSAOE-15-45_07 taken at 25kX.

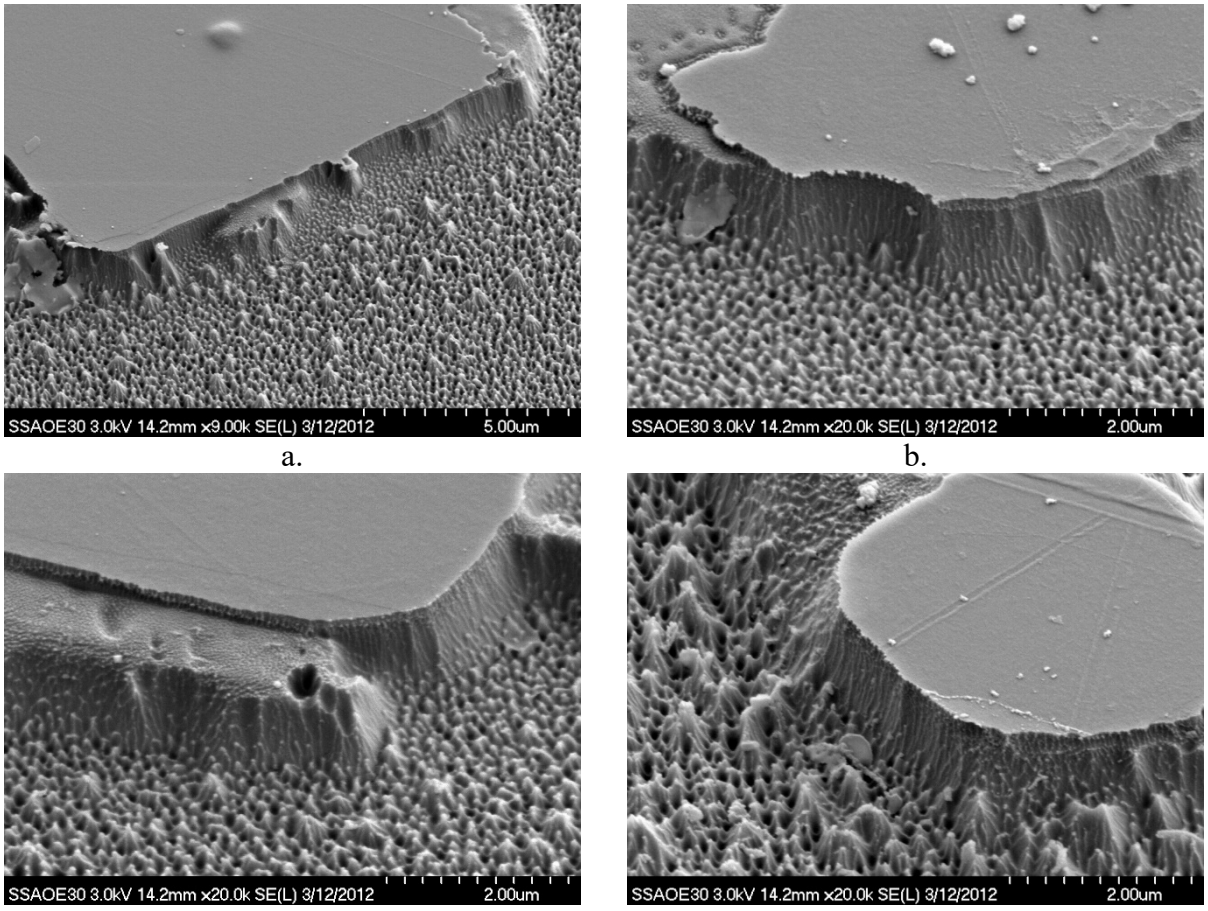

Figure 29. SEM images of salt protected buttes taken at the 30° sample angle (105° scatter angle) and at a 45° SEM title angle: (a) Image SSAOE-30-45_10 taken at 9kX, (b) Image SSAOE-30-45_12 taken at 20kX, (c) Image SSAOE-30-45_14 taken at 20kX, and (d) SSAOE-30-45_16 taken at 20kX.

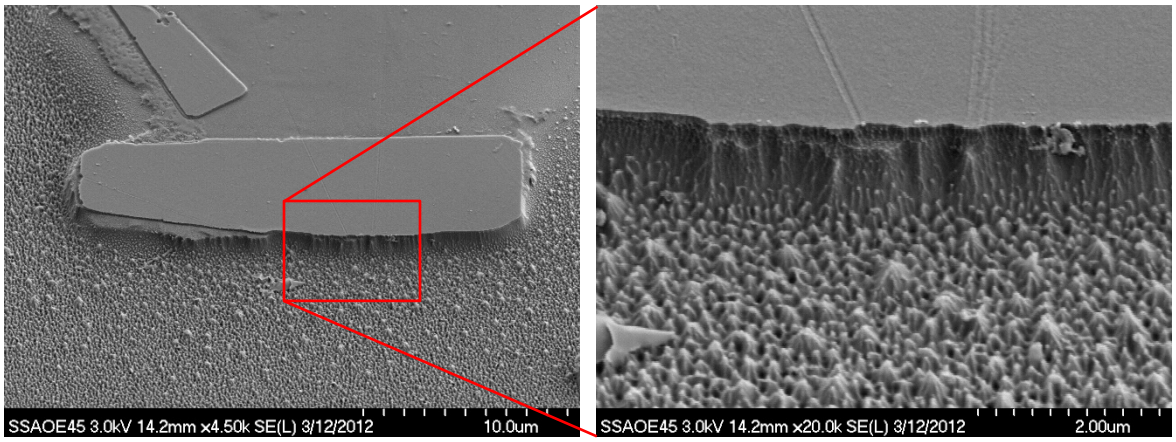

a. b.

Figure 30. SEM images of a salt protected butte taken at the 45° sample angle (90° scatter angle) and at a 45° SEM title angle: (a) Image SSAOE-45-45_03 taken at 4.5kX, and (b) Image SSAOE-45-45_04 is a close-up of the butte taken at 20kX.

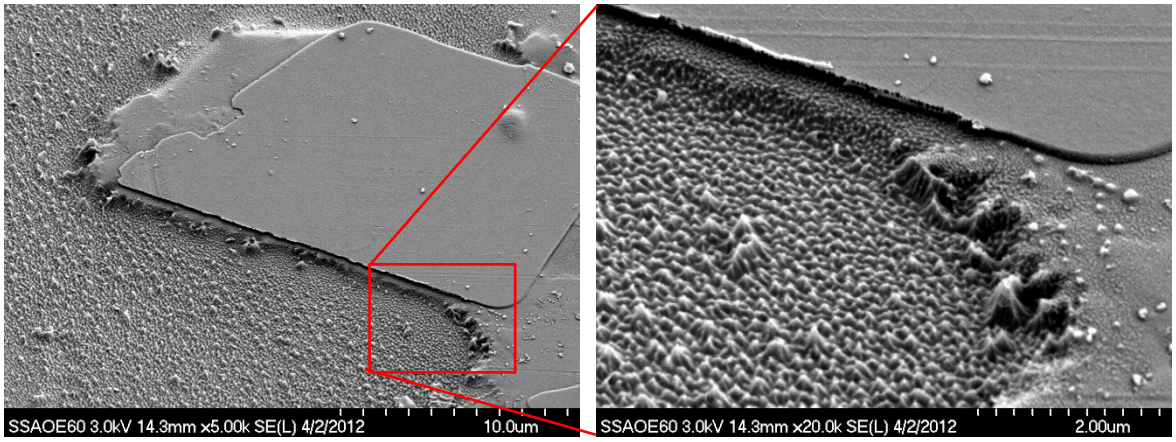

a. b.

Figure 31. SEM images of a salt protected butte taken at the 60° sample angle (75° scatter angle) and at a 45° SEM title angle: (a) Image SSAOE-60-45_08 taken at 5kX, and (b) Image SSAOE-60-45_09 is a close-up of the salt protected butte taken at 20kX.

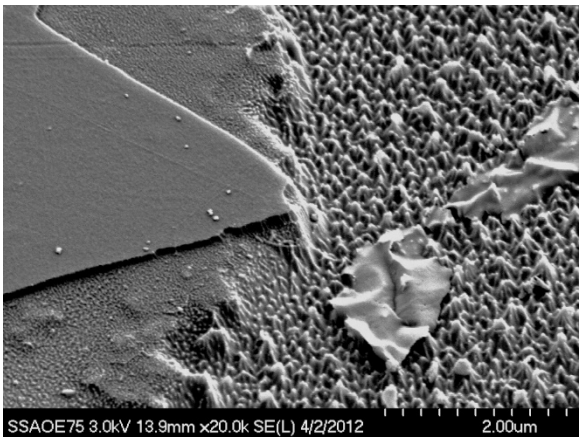

Figure 32. SEM image (SSAOE-75-45_03, 20kX) of a salt protected butte taken at the 75° sample angle (60° scatter angle) and at a 45° SEM title angle.

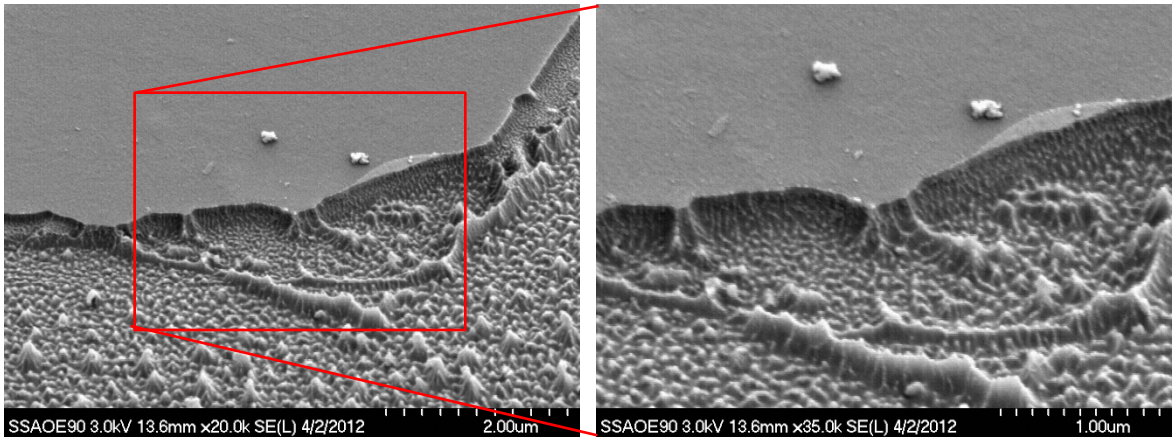

a. b.

Figure 33. SEM images of a salt protected butte taken at the 90° sample angle (45° scatter angle) and at a 45° SEM title angle: (a) Image SSAOE-90-45_02 taken at 20kX, and (b) Image SSAOE-90-45_03 is a close-up of the butte taken at 35kX.

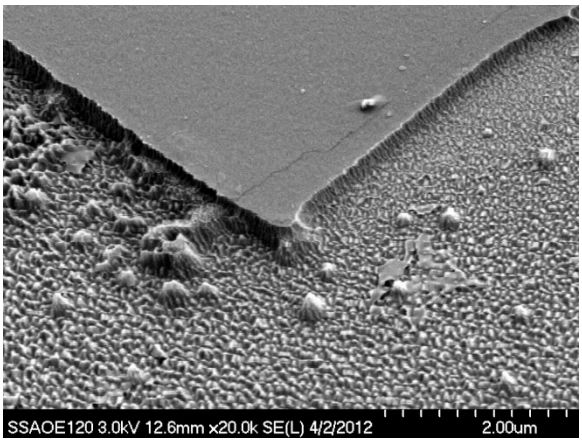

Figure 34. SEM image (SSAOE-120-45_03, 20kX) of a salt protected butte taken at the 120° sample angle (15° scatter angle) and at a 45° SEM title angle.

Results of the erosion depth versus AO scatter angle are provided in Table 3 and are visually represented in the bar graph in Figure 35. As shown in the bar graph, the greatest erosion depth occurred at a 90° scatter angle. The images, such as Figure 28a, indicate that scattering within the scattering chamber caused slight AO undercutting of the Kapton that was covered with salt particles, as would be expected. The erosion depth versus scatter angle data indicates that there was only a slight increase in erosion due to flux scattered in a forward direction which indicates that the primary ejection of AO flux is normal to the scattering surface. This is different than the results by Banks et al. in Reference 16 where the primary ejection of AO within a MISSE 2 AO scattering chamber was at 45° off an aluminum target that was exposed to normal incidence LEO AO.

Table 3. Erosion Depth vs. AO Scatter Angle.

Picture ID	Sample Angle (°)	Scatter Angle (°)	Image Mag. (kX)	Erosion Depth at 45° Tilt, d (in.)	Actual Erosion Depth, D (in.)	Length of Scale Bar (in.)	Scale Bar Unit (μm)	Actual Erosion Depth, D (μm)	Ave. Actual Erosion Depth, D (μm)	Std. Dev. Actual Erosion depth, D (μm)
SSAOE-15-45_02	15	120	20.0	1.131	1.60	3.360	2.00	0.95	1.35	0.34
SSAOE-15-45_06			25.0	2.029	2.87	4.185	2.00	1.37		
SSAOE-15-45_07			25.0	1.510	2.14	4.191	2.00	1.02		
SSAOE-15-45_08			25.0	1.913	2.71	4.204	2.00	1.29		
SSAOE-15-45_09			25.0	2.722	3.85	4.191	2.00	1.84		
SSAOE-15-45_10			20.0	1.931	2.73	3.35	2.00	1.63		
SSAOE-30-45_02	30	105	10.0	0.97	1.37	4.197	5.00	1.63	1.65	0.22
SSAOE-30-45_04			20.0	1.828	2.59	3.358	2.00	1.54		
SSAOE-30-45_07			20.0	2.013	2.85	3.418	2.00	1.67		
SSAOE-30-45_09			20.0	2.374	3.36	3.426	2.00	1.96		
SSAOE-30-45_10			9.0	0.919	1.30	3.85	5.00	1.69		
SSAOE-30-45_12			20.0	2.136	3.02	3.42	2.00	1.77		
SSAOE-30-45_14			20.0	1.517	2.15	3.423	2.00	1.25		
SSAOE-30-45_15			20.0	2.019	2.86	3.428	2.00	1.67		
SSAOE-30-45_16			20.0	1.665	2.35	3.410	2.00	1.38		
SSAOE-30-45_17			13.0	1.529	2.16	4.447	4.00	1.94		
SSAOE-45-45_04	45	90	20.0	2.002	2.83	3.362	2.00	1.68	1.68	N/A
SSAOE-60-45_07	60	75	35.0	1.812	2.56	2.94	1.00	0.87	0.87	N/A
SSAOE-75-45_03	75	60	20.0	1.4375	2.03	3.364	2.00	1.21	1.21	N/A
SSAOE-90-45_02	90	45	20.0	0.537	0.76	3.355	2.00	0.45	0.53	0.11
SSAOE-90-45_03			35.0	1.014	1.43	2.934	1.00	0.49		
SSAOE-90-45_05			10.0	0.392	0.55	4.194	5.00	0.66		
SSAOE-120-45_03	120	15	20.0	0.491	0.69	3.35	2.00	0.41	0.41	N/A

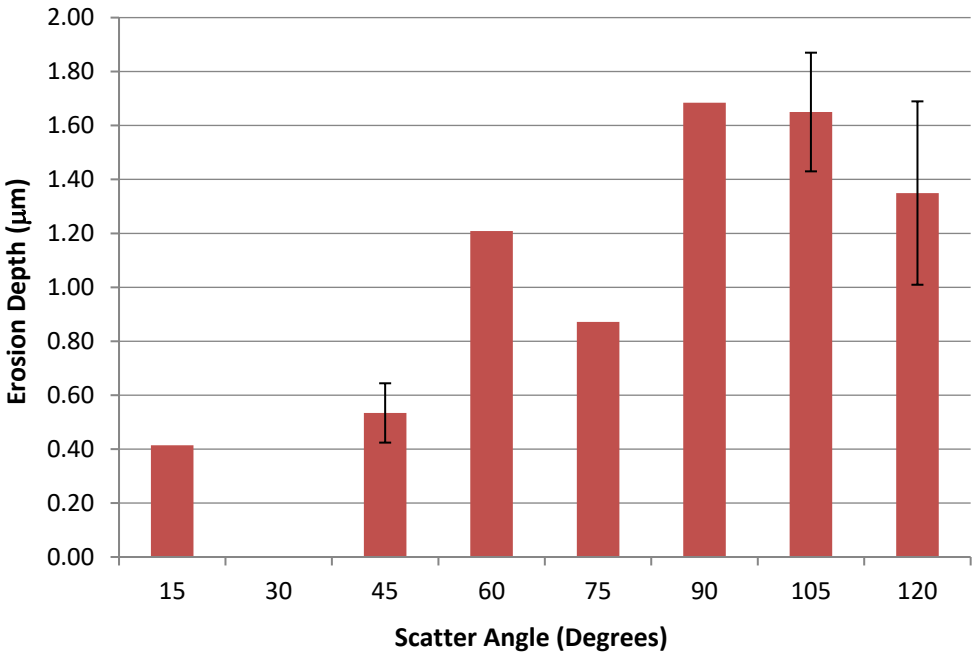

Figure 35. Bar graph showing the erosion depth versus the scatter angle.

Summary and Conclusions

The SSAOE is a flight experiment developed to characterize AO scattering erosion in space. The SSAOE is comprised of three independent sub-experiments including an active AO scatterometer, a passive AO scatterometer and passive E_y samples. The SSAOE was originally flown on the STS-60 WFS, but received very little AO during the shuttle mission. Thus, the experiment was re-flown as part of the MISSE 6 mission. During the 1.45 year MISSE 6 mission, the SSAOE was positioned in the ram direction and received an AO fluence of $1.90 \pm 0.05 \times 10^{21}$ atoms/cm^2. Unfortunately, due to a power supply problem the active experiment did not operate on-orbit as planned. Thus, only the passive sub-experiments could be analyzed post-flight. This paper provides visual degradation of the passive E_y samples and data on the angular distribution of LEO AO scattered off a fused silica slide at a 45° inclined angle.

Scanning electron microscope images were obtained of the passive AO scatterometer Kapton liner after the salt particles were removed. Images were taken at 15° scatter angles from 15° to 120°, except at a 105° scatter angle. The SEM images indicate that scattering within the scattering chamber can produce slight AO undercutting of the Kapton at the salt-protected edges, as would be expected. Kapton erosion depth measurements were made from the SEM images at salt-protected areas. The results indicate that the greatest erosion depth occurred at a 90° scatter angle from the 45° inclined fused silica slide. The erosion depth versus scatter angle data indicates that there was only a slight increase in erosion due to flux scattered in a forward direction which indicates that the primary ejection of AO flux is normal to the scattering surface. A MISSE 2 AO Scattering Chamber experiment where the primary ejection of AO within an AO scattering chamber was at 45° off an aluminum substrate that was exposed to normal incidence AO. The LEO scattered AO erosion data can be used to improve AO undercutting models and durability predictions of spacecraft components receiving scattered AO.

References

1. Dickerson, R.E., Gray, H.B., and Haight, G P., *Chemical Principles 3rd Edition*. Menlo Park, CA: Benjamin Cummings Publishing Co. Inc. p. 457, 1979.
2. de Groh, K.K., Banks, B.A. and McCarthy, C.E., *Spacecraft Polymers Atomic Oxygen Durability Handbook*. NASA–HDBK–6024, 2017.
3. National Aeronautics and Space Administration: U.S. Standard Atmosphere, 1976. NASA TM–X–74335, 1976.
4. Gregory, J.C., "Interaction of Hyperthermal Atoms on Surfaces in Orbit: The University of Alabama Experiment," David E. Brinza, Ed., *Proceedings of the NASA Workshop on Atomic Oxygen Effects*, *Nov. 10–11*, *1986*. JPL 87–14, pp. 29–30.
5. Dever, J.A., "Low Earth Orbital Atomic Oxygen and Ultraviolet Radiation Effects on Polymers," NASA TM 103711, February 1991.
6. de Groh, K.K., Banks, B.A., Miller, S.K.R., and Dever, J.A., Degradation of Spacecraft Materials (Chapter 28), Handbook of Environmental Degradation of Materials, Myer Kutz (editor), William Andrew Publishing, pp. 601–645, 2018.
7. O'Neal, R.L., Levine, A.S. and Kiser, C.C., *Photographic Survey of the LDEF Mission*. NASA SP-531. NASA LaRC: Hampton, VA (1996).
8. de Groh, K.K. and Banks, B.A., "Atomic Oxygen Undercutting of Long Duration Exposure Facility Aluminized-Kapton Multilayer Insulation," *Journal of Spacecraft and Rockets*. Vol. 31, No. 4, pp. 656–664 (July-August 1994).
9. de Groh, K.K., Banks, B.A., Dever, J.A., Jaworske, K.J., Miller, S.K., Sechkar, E.A. and Panko, S.R., "NASA Glenn Research Center's Materials International Space Station Experiments (MISSE 1-7)," Proceedings of the International Symp. on "SM/MPAC&SEED Experiment," JAXA-SP-08-015E, 2009, pp. 91–119; also NASA/TM—2008-215482.
10. Banks, B.A., de Groh, K.K., and Miller, S.K., "Low Earth Orbital Atomic Oxygen Interactions with Spacecraft Materials," Materials Research Society Symposium Proceedings 2004, NN8.1; also NASA/TM—2004-213400, November 2004.
11. de Groh, K.K. Banks, B.A. Clark, G.W. Hammerstrom, A.M. Youngstrom, E.E. Kaminski, C. Fine E.S. and Marx, L.M., "A Sensitive Technique Using Atomic Force Microscopy to Measure the Low Earth Orbit Atomic Oxygen Erosion of Polymers," presented at the Poly Millennial 2000 Conference, Kona, HI, Dec. 9–13, 2000; NASA TM-2001-211346.
12. de Groh, K.K., Banks, B.A. and Demko, R., "Techniques for Measuring Low Earth Orbital Atomic Oxygen Erosion of Polymers," Proceedings of the SAMPE 2002 Conference, Long Beach, CA, May 6–10, 2002, pp. 1279–1292; also NASA/TM—2002-211479, March 2002.
13. Center on Materials for Space Structures, Case Western Reserve University, "STS-60 MatLab-01 Materials Flight Experiment (MFLEX)," Report, April 1994.
14. de Groh, K.K., Banks, B.B., Mitchell, G.G., Yi, G.T., Guo, A., Ashmead, C.C., Roberts, L.M., McCarthy, C.E. and Sechkar, E.A., "MISSE 6 Stressed Polymers Experiment Atomic Oxygen Erosion Data," Proceedings of the ISMSE 12', Noordwijk, The Netherlands (ESA SP-705, 2013); also NASA/TM—2013-217847.
15. Pippin, H.G., Wert, J.L. and Robb, A., "MISSE-6 Post-Flight Examination, Disassembly and Analysis Results," The Boeing Company Final Report FA9550-09-C0206, Dec. 21, 2010.
16. Banks, B.A., de Groh, K.K. and Miller, S.K., "MISSE Scattered Atomic Oxygen Characterization Experiment," Proceedings of the 2006 NSMMS in conjunction with the 2006 MISSE Post-Retrieval Conference, Orlando, Florida, June 26–30, 2006; also NASA TM-2006-214355.